THE EFFECT OF THE NADPH OXIDASE *YNO1* ON TRANSLATIONAL FIDELITY

JAMES P DOWLING

A thesis submitted for the degree of Masters by Research in Cell Biology

University of Kent

School of Biosciences

August 2018

Declaration

No part of this thesis has been submitted in support of an application for any degree or other qualification of the University of Kent, or any other University or Institution of learning.

Signed: James Peter Dowling, 12th February 2019

Abstract

The hypothesized relationship between translational fidelity and ageing is complex, dating back half a century and so far represented by few known conclusions. Translational fidelity is known to remain constant with ageing, but the mechanism through which this is possible is currently a mystery. Recently, the yeast NADPH oxidase Yno1p was implicated in the regulation of translational fidelity, and the relationship between Yno1p and translational fidelity was investigated here in more detail. Through luciferase-based translational fidelity assays, here was shown that *YNO1* expression is negatively correlated with high frequency of stop-codon read-through, and this pattern is mimicked by overnight ROS exposure, providing evidence that ROS produced by Yno1p improves translational fidelity. Furthermore, *YCK1, YCK2* and *HEK2* was shown to be independently essential in mediating the fidelity improvement signal from Yno1p to the translational machinery. Additionally, the mechanism by which hydrogen peroxide exposure and Yno1p improves fidelity appears to be independent, but both can produce additive improvements in fidelity. Using growth assays, overexpression of *YNO1* and hydrogen peroxide exposure were both shown to increase sensitivity to nourseothricin (NTC), a translational error-inducing drug. *YNO1* was found to be an important regulator of translational fidelity.

Acknowledgements

The credit for my instruction on the two primary areas of theory can be split equally between my two supervisors; the *YNO1* work originating from the lab of Dr. Campbell Gourlay and the translational fidelity connection from the lab of Dr. Tobias von der Haar.

I'd like to offer my greatest appreciation to Dr. Patrick Rockenfeller for getting me started and assisting far more than he was required to do in teaching me proper laboratory practice and the primary techniques used in this thesis.

I'd also like to thank several lab members at the University of Kent for their share of assistance, which saved me many work hours in the limited timeframe I had to complete this project, most prominently: Jack Davis, Bradley Vincent and Dr. Nadia Koloteva-Levine.

Table of Contents

Table of Figures

Table of Tables

1 Introduction

1.1 The Mechanism of Translation

1.1.1 Overview of Translation

The cell devotes more energy to protein synthesis than any other process (Buttgereit and Brand, 1995); while rapidly growing, *Saccharomyces cerevisiae* synthesises an estimated 13,000 protein molecules per second (von der Haar, 2008) and 2000 ribosomes per minute (Warner, 1999), with 15,000 – 60,000 mRNA transcripts present at any one time to be translated (Zenklusen, Larson and Singer, 2008). However, despite its great significance to the cell, translation is not a completely accurate process. Mistakes are made which contribute to a decline in cell fitness, and associated with this are various diseases. In this introduction an overview is provided of the mechanism of eukaryotic translation, an outline of the steps which are error-prone, as well as a description of the significant consequences of translational infidelity, both at the resolution of the cell and of the organism with a particular focus on age-related diseases.

Translation is the process of decoding the information stored in the codon sequence of mRNA and using it to synthesise a protein of corresponding amino acid sequence. The process can be broadly broken down into three discrete steps: an 80S ribosome is assembled and the first codon is decoded during initiation; the remaining codons are decoded during elongation, and the resultant polypeptide is released during termination.

1.1.2 Initiation

Initiation describes the assembly process of an 80S ribosome and its subsequent decoding of an AUG start codon on a strand of mRNA by facilitating pairing with the anticodon of a methionyl initiator tRNA (Met-tRNAi^{Met}) (Figure 1).

The process begins with a 40S ribosomal subunit binding three translation initiation factors (eIFs): eIF1, eIF1a and eIF3. This complex then binds a ternary complex consisting of eIF2 bound to GTP and Met-tRNAi^{Met}. This tRNA is charged with methionine and its anticodon is complementary to the AUG start codon. The two complexes then bind a molecule of eIF5, resulting in the formation of the 43S pre-initiation complex (PIC) (Dever, Kinzy and Pavitt, 2016).

A molecule of mRNA is activated once bound to a multitude of proteins, including eIF4E at the 5' cap and Pab1 at the Poly(A) tail. These two proteins are bridged by eIF4G, curling the mRNA into a loop structure (Wells *et al.*, 1998). eIF4A and eIF4B also bind the activated mRNA. The 43S PIC is then able to bind the activated mRNA close to the 5' cap. The resulting structure is the 48S complex (Pestova and Kolupaeva, 2002).

Following this is a process known as scanning, whereby the 43S PIC moves in a 5' to 3' direction along the 5' UTR of the mRNA in search of an AUG start codon. Once reached and recognised by the anticodon of the Met-tRNAi^{Met}, the GTP bound to eIF2 is hydrolysed, and the resulting eIF2 and Pi are released, along with eIF1 and eIF5 (Hinnebusch, 2014). Following this, the 60S subunit binds the 48S complex, facilitated by the hydrolysis of GTP bound to eIF5B (Pestova *et al.*, 2000). The resulting eIF5B-GDP is released, along with eIF1A. The remaining structure is the 80S ribosome bound to a molecule of mRNA, with Met-tRNAi^{Met} in the P site (Dever, Kinzy and Pavitt, 2016).

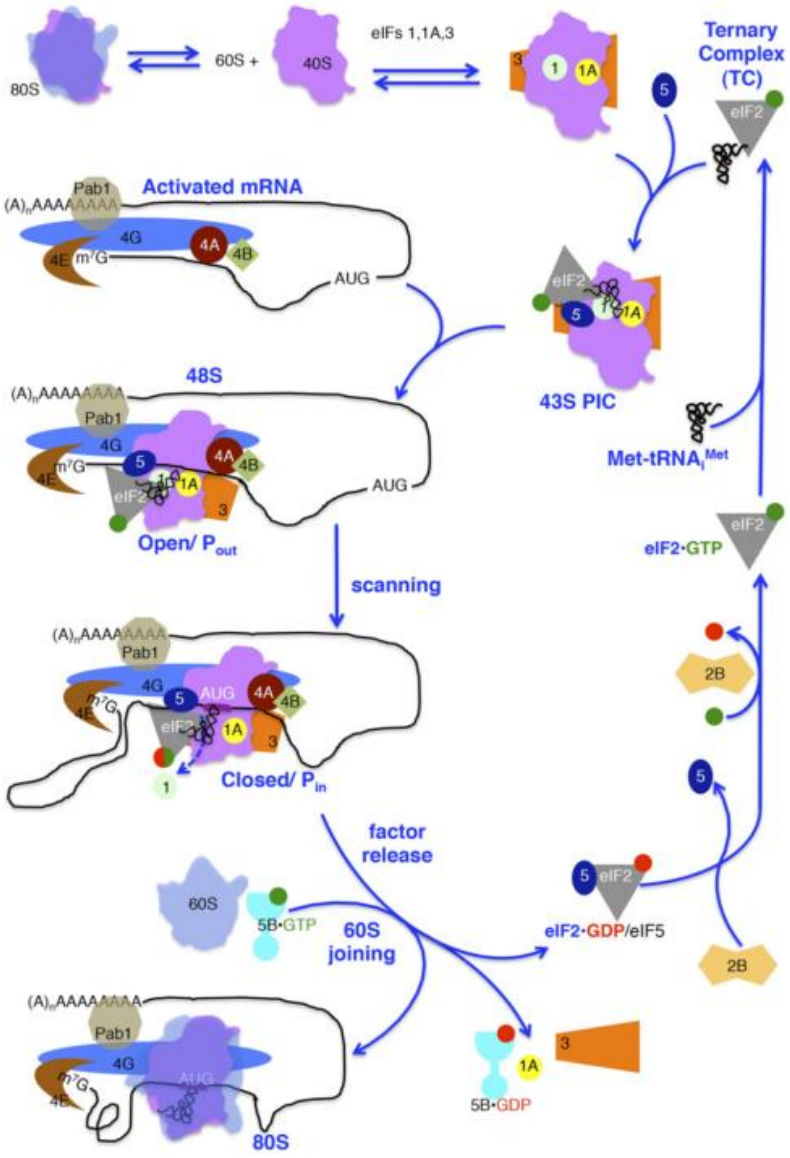

***Figure 1**: Mechanism of Translation Initiation*

Two complexes, one consisting of a 40S subunit, eIF1, eIF1a and eIF3, and the other consisting of eIF2, GTP and Met-tRNAi^{Met} bind eIF5 to form the 43S PIC. Separately, mRNA is activated through binding of eIF4E, Pab1, eIF4G, eIF4A and eIF4B. The 43S PIC and activated mRNA bind together, and the former moves along the latter in a 5' to 3' direction in a process known as scanning until the AUG start codon is recognized by the Met-tRNAi^{Met}. The GTP bound to eIF2 is hydrolyzed, and the resultant eIF2 and Pi are released, along with eIF1 and eIF5. The 60S subunit then binds the complex facilitated by the hydrolysis of GTP bound to eIF5B. The resulting eIF5B-GDP is released, along with eIF1A. The final structure is the 80S ribosome bound to mRNA. (Dever, Kinzy and Pavitt, 2016)

1.1.3 Elongation

Elongation is a series of repeating reactions that decode the codon sequence in a 5' to 3' direction to synthesise a polypeptide (Figure 2).

A ternary complex of an aminoacyl-tRNA, that is a tRNA charged with an amino acid, bound to eukaryotic elongation factor (eEF) eEF1A and GTP binds the A site of the 80S ribosome. Specifically, the codon of the mRNA and anticodon of the aa-tRNA are matched in the decoding centre of the ribosome (Noller, 2006). If the aa-tRNA is cognate then the GTP is hydrolysed. The remaining eEF1A-GDP is released, leaving just the aa-tRNA in the A site (Dever, Kinzy and Pavitt, 2016).

The peptidyl transferase centre (PTC) on the ribosome positions the aa-tRNA in the A site and the peptidyl-tRNA in the P site in energetically favourable conditions (Sievers *et al.*, 2004), and because of this a peptide bond immediately forms between the amino acid of the aa-tRNA and the terminal amino acid of the peptidyl-tRNA. In the process, the peptide is transferred from the tRNA in the P site to the tRNA in the A site, leaving the former deacylated (Rodnina and Wintermeyer, 2009).

Following this, the ribosomal subunits ratchet relative to each other, causing the tRNA molecules bound to the A and P sites to occupy both the A and P or P and E sites respectively. Binding of eEF2-GTP, and subsequent hydrolysis of this GTP, remedies the existence of these hybrid states by translocating the anticodon loops into the new sites. The deacylated tRNA is released from the E site, leaving a new ternary complex free to bind the A site, propagating the cycle of elongation (Rodnina and Wintermeyer, 2009).

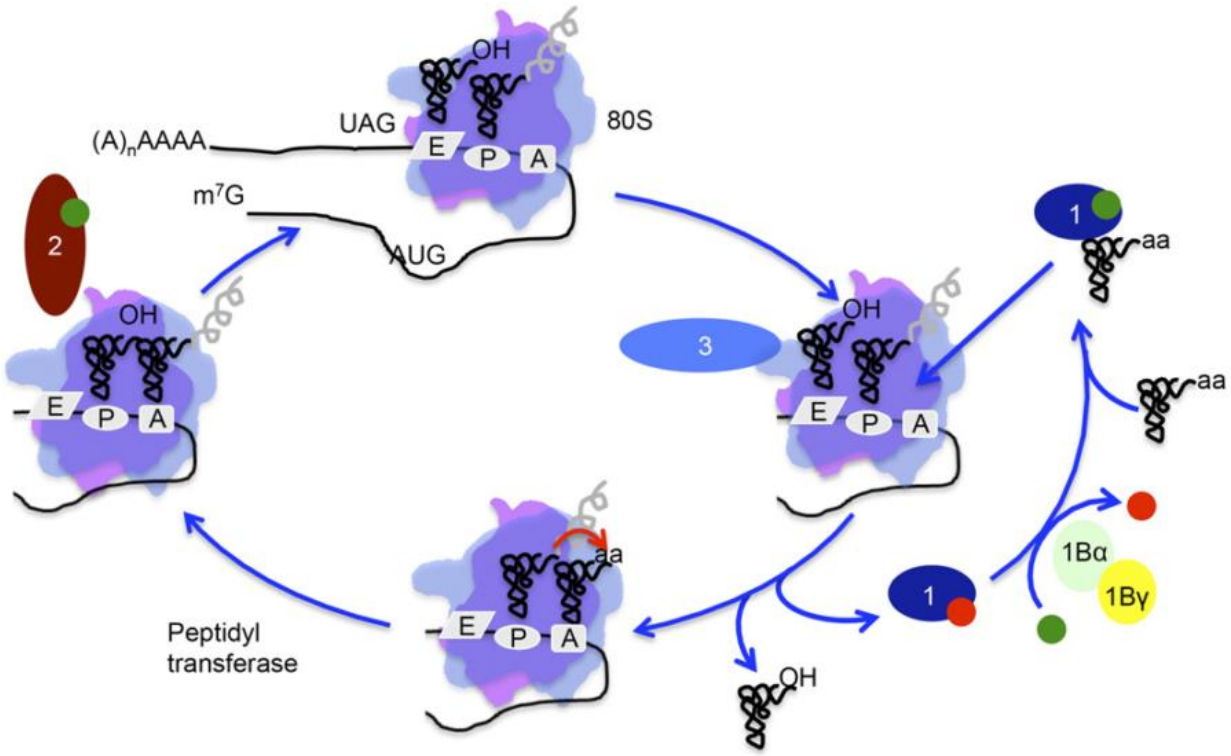

***Figure 2**: Mechanism of Translation Elongation*
A complex consisting of an aa-tRNA, eEF1A and GTP binds the A site. If the aa-tRNA is cognate, the GTP is hydrolyzed. Peptidyl transfer occurs whereby a peptide bond forms between the aa-tRNA in the A site and the peptidyl-tRNA in the P site and the peptide is transferred from the tRNA in the P site to the tRNA in the A site. The ribosome ratchets, and with assistance from eEF2-GTP, the now deacylated tRNA in the P site translocates to the E site and the now peptidyl-tRNA translocates to the P site. (Dever, Kinzy and Pavitt, 2016)

1.1.4 Termination

Termination is the cessation of elongation and the release of the polypeptide chain from the peptidyl-tRNA once a stop codon is reached by the ribosome (Figure 3).

A complex consisting of two eukaryotic release factors (eRFs), eRF1 and eRF3, and a molecule of GTP forms and binds the ribosome (Mitkevich *et al.*, 2006). GTP is hydrolysed by eRF3, which positions eRF1 in the PTC (Salas-Marco and Bedwell, 2004) where it recognises one of the three stop codons (Bertram *et al.*, 2000). eRF3 then dissociates, and Rli1/ABCE1 binds eRF1 in the PTC. This promotes the hydrolysis of the peptidyl-tRNA bond by eRF1, subsequently leading to release of the polypeptide (Shoemaker and Green, 2011).

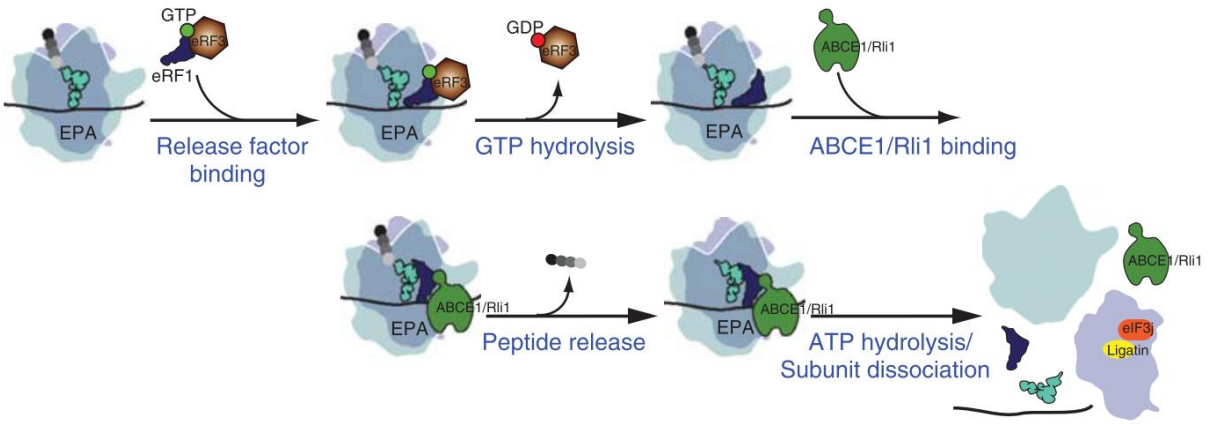

Figure 3: *Mechanism of Translation Termination*

A complex consisting of eRF1, eRF3 and GTP binds the ribosome. The GTP is hydrolyzed to aid in stop codon recognition by eRF1, and eRF3 dissociates. Rli1/ABCE1 binds eRF1, and this promotes hydrolysis of peptidyl-tRNA bond by eRF1. The polypeptide is thus released. (Dever and Green, 2012)

1.2 Translational Fidelity

1.2.1 Overview of Translational Fidelity

Translation is an imperfect process; a substantial number of proteins contain at least one error (Drummond and Wilke, 2008). The overwhelming majority of these errors occur during decoding of the mRNA codon sequence, with the resultant error classified as either missense, where an incorrect amino acid is built into the polypeptide, or nonsense suppression, where a stop codon is incorrectly interpreted as a sense codon (Zaher and Green, 2009a; Ke *et al.*, 2017). Other sources of errors include misacylation of tRNA before their involvement in translation, which cause missense errors, and shifts in the ribosomal frame, which cause frameshift errors.

Missense error rate is in the range of 10^{-3}-10^{-6} in yeast, depending on the codon (Stansfield *et al.*, 1998; Kramer and Farabaugh, 2007; Kramer *et al.*, 2010) and nonsense suppression error rate occurs at a frequency of 10^{-3}-10^{-5} (Keeling *et al.*, 2004). These are low, but not statistically insignificant.

1.2.2 Errors and Proofreading during Decoding

A codon and anticodon consist of three nucleotides. A tRNA is termed ‘cognate’ to a specific codon if Watson-Crick pairing exists at nucleotides 1 and 2, with either Watson-Crick pairing or a wobble at position 3. A tRNA is ‘non-cognate’ if there is a mismatch at position 1 or 2. Finally, a tRNA is typically called ‘near-cognate’ if there is Watson-Crick pairing at positions 1 and 2, but a mismatch at position 3 (Plant *et al.*, 2007; Atkins and Bjork, 2009). The ribosome is able to discriminate between cognate and near/non-cognate aa-tRNAs, albeit imperfectly (Parker, 1989).

Decoding accuracy is determined by kinetic, energetic and geometric mechanisms at multiple selection stages: preferential incorporation of cognate aa-tRNAs during initial selection before GTP hydrolysis (Schmeing *et al.*, 2009); preferential rejection of near-cognate aa-tRNAs during proofreading after GTP hydrolysis (Rodnina *et al.*, 2005) and preferential release of near-cognate peptidyl-tRNAs by the termination factors (Zaher and Green, 2009b).

Geometry

Selection for the cognate aa-tRNA begins with the binding of the anticodon of the aa-tRNA to the preformed decoding centre. If the tRNA is non-cognate then it will not bind (Rozov *et al.*, 2016).

Cognate and near-cognate aa-tRNAs both stimulate the 40S subunit to undergo an identical conformational change, the result of which is the formation of the decoding centre. This constrains the mRNA so that the nucleotides at position 1 and 2 of the codon in the A site are restricted geometrically to form only Watson-Crick pairs. This causes near-cognate aa-tRNAs to dissociate due to mismatches (Demeshkina *et al.*, 2012). However, some mismatches will be close enough to Watson-Crick geometry to avoid being forced to dissociate (Manickam *et al.*, 2016). Examples of this discrimination are the non-canonical pairs C-A and G-U, where the former does not conform to Watson-Crick geometry and is not accompanied in the decoding centre (Rozov *et al.*, 2015) whilst the latter does conform and is allowed to remain (Demeshkina *et al.*, 2012). Additionally, if the near-cognate anticodon is protonated or in a rare tautomeric state, it may also conform to the restricted geometry and pass this checkpoint (Rozov *et al.*, 2016).

GTPase activation

In order for elongation to progress, GTP in the ternary complex must be hydrolysed. If the aa-tRNA in the decoding centre is cognate, then the rate of GTPase activation increases by many orders of magnitude (Noller, 2006). This is because the free energy of binding (Zaher and Green, 2009a) induces conformational changes in the decoding site, which leads to conformational changes in the 40S subunit (Ogle *et al.*, 2002). This acts as a signal for the GTPase centre on the 60S subunit to accelerate the preceding steps before GTP hydrolysis (Rodnina and Wintermeyer, 2009). A near-cognate aa-tRNA won't induce these conformational changes (Ogle *et al.*, 2002), and so rate of GTP hydrolysis will be lower. This increases the likelihood of it dissociating from ribosome (Schmeing *et al.*, 2009).

Proofreading

There are two proofreading steps during elongation. The first is immediately following GTP hydrolysis, where the aa-tRNA can either be accommodated in the A site of the ribosome and participate in peptidyl transfer, or dissociate. The rate of the former is favored by cognate aa-tRNAs, whereas the rate of the latter is favored by near-cognate aa-tRNAs (Rodnina *et al.*, 2005).

Kinetic Proofreading

The ribosome uses the enzymatic mechanism of kinetic proofreading to boost the accuracy of aa-tRNA selection; when two selection steps are separated by an irreversible step in the reaction pathway, then the overall accuracy of selection increases exponentially proportional to the number of selection steps (Hopfield, 1974; Ninio, 1975). In the context of translation, this is the utilisation of the small differences in binding energy between cognate and near-cognate aa-tRNAs to discriminate between them both before and after irreversible GTP hydrolysis. The step

preceding and following hydrolysis both contribute at comparable magnitudes to the accuracy of selection (Gromadski and Rodnina, 2004).

Stop-codon read-through

When a stop codon is in the A site, there is competition between the termination and elongation apparatus, which are essentially release factors and aa-tRNAs respectively. If the fidelity of either set of machinery decreases, then the stop codon could be paired with an aa-tRNA, and elongation would continue past the stop codon (Salas-Marco and Bedwell, 2005).

1.2.3 Aminoacylation

Aminoacyl-tRNA synthetases (aaRSs) catalyse the charging of a tRNA with an amino acid. These are highly specific enzymes, however they occasionally pair the wrong amino acid and tRNA. This is remedied by the editing function of these enzymes, which cleave off the incorrect amino acid (Ling, Roy and Ibba, 2007). The accuracy of this process is very high; errors occur at a frequency in the range of 10^{-4} – 10^{-6} depending on the editing capability of the specific aaRS (Söll, 1990; Ibba and Söll, 2000; Francklyn, 2008).

The accuracy of aminoacylation is maintained due to multiple factors. If the amino acid and tRNA are not a correct pair, then either they will not bind the enzyme due to the principles of induced fit, or the catalytic efficiency is poor due to poorly aligned geometry of the reacting groups. If a tRNA is still charged with the wrong amino acid then the editing function of the aaRS is employed. This is a deacylation reaction which occurs at a separate domain to the catalytic domain. This is carried out at high accuracy through the ‘double sieve’ mechanism, which effectively removes amino acids smaller than the intended correct one, as well as other

mechanisms involving selection through geometry, hydrogen bonding and electrostatic forces (Francklyn, 2008).

eEF1A is able to discriminate between correctly and incorrectly aminoacylated tRNAs, providing another level of control (LaRiviere, 2001).

1.2.4 Ribosomal Frame Shifting

As the codon sequence that constitutes mRNA is decoded three nucleotides at a time, information can be read in three frames. If the ribosome moves forward or backwards one nucleotide during translation, the whole frame changes, as each three nucleotide codon would be read differently. Failure to maintain frame leads to erroneous peptides being synthesised, or a stop codon will be created by the new frame and translation will be terminated (Atkins and Bjork, 2009). Ribosomal frame shifting is kept at the low frequency of 10^{-4} - 10^{-5} (Jørgensen and Kurland, 1990; Atkins, 1991), and this is because all peptides produced by losing frame are irredeemably incorrect (Atkins and Bjork, 2009).

The rate of frame shifting is highly linked to an imbalance in the relative quantities of aa-tRNAs. A sparse quantity of cognate aa-tRNA leads to a stall in translation, allowing the peptidyl-tRNA in the P site to dissociate from the mRNA and bind again in a different frame (Atkins and Bjork, 2009). As a result, the rate of frameshift errors may be higher than previously thought; during the proofreading step that follows peptidyl transfer (Zaher and Green, 2009b), translation halts if the aa-tRNA is not cognate, predisposing the ribosome to frameshift (Maehigashi *et al.*, 2014).

The most common cause of a frame shift is the incorporation of a frameshift suppressor tRNA into the decoding site (Farabaugh, 2000). These are tRNAs with a nucleotide insert in the

anticodon, and most commonly specify the frame to shift by +1. The ribosome, due to the previously described geometric restrictions of the decoding centre, only allow decoding of three nucleotides at any given time. As such, the four nucleotide anticodon of a suppressor tRNA probably causes the P site to undergo a rearrangement and in doing so shift frame (Maehigashi *et al.*, 2014).

Ribosomal frame shifting is also highly linked to incorporation of near-cognate aa-tRNAs in the decoding centre, where the weaker the binding energy the more the ribosome is encouraged to frame shift (Farabaugh and Björk, 1999).

1.3 Consequences of Infidelity

1.3.1 Cell Health

In eukaryotes, at the quoted error rate of 10^{-3}-10^{-6}, 15% of average-length protein molecules will contain at least one missense error (Drummond and Wilke, 2009). Of these, approximately one third will result in dysfunctional or misfolded proteins (Schubert *et al.*, 2000; Guo, Choe and Loeb, 2004). Most mutations that render loss of function to the protein do so via impairing its ability to fold correctly. In addition, the misfolded molecules possess inherent generic cytotoxicity (Bucciantini *et al.*, 2002). Misfolded proteins have a tendency to form insoluble aggregates due to the fact that hydrophobic residues, which would normally be hidden in the native protein, are exposed and bind two misfolded proteins together (Drummond and Wilke, 2009).

There are many direct toxic effects of misfolded proteins, including inhibition of the proteasome, initiating alterations to autophagy (Ross and Poirier, 2005), and inducing cellular stress

responses (Ribas de Pouplana *et al.*, 2014). Aggregates also disrupt the integrity of cell membranes, leading to oxidative stress and increases in free intracellular Ca^{2+}, leading typically to apoptosis or necrosis (Stefani and Dobson, 2003). An accumulation of misfolded proteins in the endoplasmic reticulum (ER), where many proteins destined for the cell surface membrane or for secretion are processed, results in the unfolded protein response to avoid ER stress. If this response is maintained for too long, the cellular quality control system is overwhelmed and the cell dies (Rao and Bredesen, 2004).

Misfolded proteins are also an indirect fitness cost to the cell, as they lead to a reduction in growth rate due to the allocation of resources to the production and processing of the misfolded proteins. For example, the ATP and proportion of total ribosomal capacity used to produce them are wasted (Stoebel, Dean and Dykhuizen, 2008). These costs are substantial, and increase in a faster-than-linear fashion with the quantity of misfolded protein produced (Dekel and Alon, 2005).

There are tight evolutionary constraints on keeping rates of infidelity low (Drummond and Wilke, 2008), the most stark of which is the observation that fidelity co-evolves with longevity (Ke *et al.*, 2017). Indeed, high levels of mistranslation are incompatible with healthy ageing (von der Haar *et al.*, 2017). However, mRNA mistranslation is also potentially adaptive. For example, genetically enhancing mRNA mistranslation rates in various unicellular organisms results in a selective fitness advantage, possibly through upregulating the expression of stressor proteins or by initiating stress-induced mutagenesis which increases the probability of adaptation by natural selection (Ribas de Pouplana *et al.*, 2014).

1.3.2 Disease

Proteins containing missense errors are a cause of pathology; evidence for this are genetic diseases caused by uncommon triplet sequences at the genetic level, as the encoded protein is the means through which pathogenesis is mediated (Drummond and Wilke, 2008). Age-related diseases, such as neurodegeneration and cancer, are of particular concern at the present time in the western world due to an ageing population, and so particular attention has been drawn to these.

Misfolded proteins are a hallmark of more than 20 (Stefani and Dobson, 2003) age-related diseases, including Alzheimer's disease, Parkinson's disease, Huntington's disease, spinocerebellar ataxias and many others (Ross and Poirier, 2004). Neurodegeneration as a class of diseases involve protein misfolding in a disproportionately high amount (Soto, 2003). This is because neurons are post-mitotic; as they are unable to divide, any misfolded proteins remain within the one cell rather than being diluted into two daughter cells during mitosis (Ross and Poirier, 2004; Lee *et al.*, 2006). In addition, neurons are relatively long, creating a high surface area to volume ratio, and hence there is a greater opportunity for misfolded proteins to damage the cell surface membrane (Kourie and Henry, 2002).

Disruption of chaperone function in the ER of terminally differentiated neurons causes neurodegeneration through aggregation of misfolded proteins and ER stress (Zhao *et al.*, 2005). Additionally, misacylation has been shown to directly cause neurodegeneration in mice; a mutation that renders the editing function of alanyl-tRNA synthetase non-functional causes levels of misacylated tRNAs to increase, consequently causing Purkinje cell loss and ataxia. This is direct evidence of translational infidelity causing neurodegeneration. In addition, the

same study hypothesised that, as the editing domain of aaRSs is separate from the catalytic domain, mutations in the former could be inherited without gross disruption of protein synthesis, suggesting that perhaps some inherited diseases could be caused by mutations in the editing domain (Lee *et al.*, 2006).

The rate of translation is one of the main determinants of cell proliferation rate (Dua, 2001). As such, translation is known to contribute to the pathogenesis of cancer (Cuesta, Gupta and Schneider, 2009), and decreased translational fidelity is associated with tumour progression (Belin *et al.*, 2009).

Mutations in genes that directly affect synthesis and processing of tRNAs have been linked to many other diseases besides the age-related ones covered here (Abbott, Francklyn and Robey-Bond, 2014). For example, multiple sclerosis could be aggravated by misacylation of tRNAs with a proline analogue, resulting in the synthesis of a protein containing a residue that is not an amino acid, which would clearly create a deficiency in folding capacity (Rubenstein, 2008). Translational infidelity also affects the mitochondria. Mutations in mitochondrial tRNA are a cause of multiple diseases. For example, a mutation in the mitochondrial tRNALys gene is the most common cause of Myoclonus Epilepsy with Ragged Red Fibers (MERRF), and a mutation in the tRNAIle gene is associated with cardiomyopathy (Rötig, 2011).

1.4 Fidelity and Ageing

1.4.1 Reactive Oxygen Species (ROS)

It has long been hypothesized that major mediators of cellular ageing are reactive oxygen species (ROS). These are molecules and free radicals composed entirely or in part of oxygen,

and due to their highly reactive nature they play a prominent role in many cellular processes, including cell signalling in cell division and stress responses (Chiu and Dawes, 2012). It is thought that intracellular ROS levels must be kept under strict redox homeostatic control; too high, and the intracellular environment becomes too volatile for any regulative processes to occur, or alternatively too low and the cell loses an important signalling mediator. The most prominent form of ROS is superoxide (O_2^-), which is produced by leakage of electrons from the electron transport chain and from the NADPH oxidase YNO1p (Rinnerthaler *et al.*, 2012). Another important form of ROS is hydrogen peroxide (H_2O_2), which is generated primarily by dismutation of superoxide by superoxide dismutase enzymes (SOD enzymes) (Ayer, Gourlay and Dawes, 2014).

1.4.2 Ageing and ROS

Ageing is generally defined as a time-dependent functional decline in physiological integrity (López-Otín *et al.*, 2013). It is a major contributor to the risk of developing pathology in humans. Ageing is characterised by several hallmarks, including mitochondrial dysfunction, loss of proteostasis and telomere attrition. One of the most popular, and controversial, theories purported to have elucidated the cause of the ageing process is the free radical theory of ageing (Harman, 2003), which briefly states that mitochondrial ageing causes ROS to be produced, which causes mitochondrial dysfunction, which in turn produces more ROS, leading to a cycle of cellular functional decline. Since this theory was put forward in 1956, ROS has been generally seen as a contributor to ageing. However, recent evidence has questioned the orthodoxy of this theory. For example, ROS was shown to potentially increase the lifespan of yeast (Mesquita *et*

al., 2010), and genetically increasing ROS production from the mitochondria has no impact of the rate of ageing (Zhang *et al.*, 2009).

1.4.3 Ageing and Translational Fidelity

Translational fidelity has long been discussed as a potential cause, or result of, the ageing process. A prominent early hypothesis was the 'error catastrophe' theory (Gallant *et al.*, 1997). It proposes that, as translational is not a completely accurate process, over the course of the life of a cell the magnitude of non-canonical gene products increases up until a 'catastrophic' point where the magnitude of errors becomes so great that the canonical peptide cannot be produced. The major challenge to this theory is that error levels have been demonstrated to remain constant during ageing across stages in lifespan and across organisms (Harley *et al.*, 1980; Stahl *et al.*, 2004). This opens up a new area of investigation – why does accuracy remain constant when the high ROS levels of the ageing cell should act to decrease translational fidelity (Mohler and Ibba, 2017)?

Yno1p, a recently discovered NADPH oxidase in yeast, has been implicated as a potential regulator of translational fidelity during ageing (von der Haar *et al.*, 2017).

1.4.4 Yeast NADPH Oxidase 1 (YNO1)

Yno1p is the only functional NADPH oxidase (NOX) in *Saccharomyces cerevisiae*, being an ortholog to human *NOX5* (Rinnerthaler *et al.*, 2012). Localised to the perinuclear endoplasmic reticulum, it catalyses a reaction which results in the production of approximately 20% of the reactive oxygen species (ROS) production in the cell under exponential growth.

Stoichiometrically, it catalyses the reversible reaction of NADPH (reduced form) with two molecules of molecular oxygen to produce NADP+ (oxidised form), a proton (H^+), and two superoxide free radicals (O_2^-) (Nauseef, 2008).

The primary product from the reaction is superoxide, which is metabolised to a further product, most frequently hydrogen peroxide (Rinnerthaler *et al.*, 2012). ROS produced by NOX enzymes is known to be an important signalling mediator. (Nauseef, 2008). Two pathways Yno1p is known to play a role in are apoptosis and starting new cell cycles (Rinnerthaler *et al.*, 2012).

Most significantly for investigation here is the link between Yno1p and mitochondrial dysfunction, one of the hallmarks of ageing, which is characterised by depolarisation of the mitochondrial membrane. This causes RAS, one of the main proliferative signalling molecules in the cell, to localise here, which constitutively signals to *YNO1* to produce superoxide (Leadsham *et al.*, 2013).

Additionally, interference in the mitochondrial electron transport chain at the genetic level causes an increase in amino acid misincorporation and a decrease in stop-codon read-through. Deleting *YNO1* under these conditions abrogates these alterations in translational fidelity, showing that Yno1p is the mediator of fidelity change under conditions of mitochondrial dysfunction, presumably through the local release of the superoxide it produces. Additionally, deletion of the *RAS2* gene, one of the mediators in the signalling pathway from the mitochondrial membrane to Yno1p, also increases translational infidelity, again supporting the above hypothesis (von der Haar *et al.*, 2017).

1.4.5 Hypothesis

The functions of Yno1p identified by Leadsham (2013) and von der Haar (2017) lend themselves to an intriguing hypothesis – is Yno1p responsible for the maintenance of translational fidelity in the face of cellular alterations that would otherwise work to the cell's physiological detriment during ageing, via Yno1p's role as the booster of intracellular ROS levels when mitochondrial dysfunction occurs?

As such, the subject of this study was to investigate the role of Yno1p in fidelity maintenance and alteration in the important context of ageing.

2 Materials and Methods

2.1 Materials

2.1.1 Table 1: Buffers

Buffer	Concentration / pH	Ingredients	Source
TAE	40mM, pH 8.3	Tris	Fisher
	20mM	Acetic Acid	Sigma
	1mM	EDTA	Sigma
TE	10mM, pH 8	Tris	Fisher
	0.1mM	EDTA	Sigma
PBS	137mM	Sodium Chloride	Fisher
	2.7mM	Potassium Chloride	Sigma
	10mM	Disodium phosphate	Sigma
	1.8mM	Monopotassium phosphate	Sigma
NEBuffer™ 2	10x stock	Proprietary	New England Biolabs

2.1.2 Table 2: Media

Medium	Final Concentration	Ingredients	Source
YPD	1% (m/v)	Yeast Extract	Bacto
	2% (w/v)	Peptone	Bacto
	$4x10^{-3}$% (m/v)	Adenine	Sigma

	2% (m/v)	Glucose	Fisher
	98% (v/v)	dH_2O	Fisher
YPD-G418	1% (m/v)	Yeast Extract	Fisher
	2% (w/v)	Peptone	Bacto
	4x10-3% (m/v)	Adenine	Sigma
	2% (m/v)	Glucose	Bacto
	98% (v/v)	dH_2O	Fisher
	$20x10^{-3}$% (m/v)	G418	Melford
SD-HIS	0.675% (m/v)	Yeast Nitrogen Base (without amino acids)	Bacto
	0.057% (m/v)	Amino acids (-HIS)	Formedium
	2% (m/v)	40% glucose	Fisher
SD-URA	0.675% (m/v)	Yeast Nitrogen Base (without amino acids)	Bacto
	0.19% (m/v)	Amino acids (-URA)	Formedium
	2% (m/v)	40% glucose	Fisher
SD-HIS/URA	0.675% (m/v)	Yeast Nitrogen Base (without amino acids)	Bacto
	0.185% (m/v)	Amino acids (-HIS, -URA)	Formedium
	2% (m/v)	Glucose or Galactose	Fisher
SD-HIS/LEU	0.675% (m/v)	Yeast Nitrogen Base (without amino acids)	Bacto
	0.155% (m/v)	Amino acids (-HIS, -LEU)	Formedium

	2% (m/v)	40% glucose	Fisher
LB	1% (m/v) 0.5% (m/v) 1% (m/v)	Tryptone Yeast Extract Sodium Chloride	Bacto Bacto Fisher
LB-Amp	1% (m/v) 0.5% (m/v) 1% (m/v) $15x10^{-3}$% (m/v)	Tryptone Yeast Extract Sodium Chloride Ampicillin	Bacto Bacto Fisher Melford
5-FOA	2% (m/v) 0.17% (m/v) 0.5% (m/v) 0.1% (m/v) $5x10^{-3}$% (m/v)	Glucose Yeast Nitrogen Base (without amino acids or ammonium sulphate) Ammonium Sulphate 5-Fluoroorotic Acid (5-FOA) Uracil	Fisher Formedium Fisons Formedium Sigma

When plates have been made, 2% (m/v) agar (Difco) was added to the mix before autoclaving. Glucose, galactose, ampicillin and G418 were added after autoclaving and cooling media to 50^{o}C. Specific instructions on making 5-FOA plates are in section 2.2.8. SD-HIS/URA + 2% glucose and +2% galactose were both used.

2.1.3 Table 3: Chemical reagents used and their source

Chemical Reagent	**Source**
Agarose	Melford
Ethanol	Fisher
Nourseothricin	Melford
2',7'-dichlorodihydrofluorescein diacetate (H_2DCFDA)	Fisher
Lithium Acetate	Sigma
Poly(ethylene glycol) – 4,000	Sigma
Ethidium Bromide	Fisher
Agar	Difco
Single Stranded DNA (Salmon Sperm)	Fisher
Passive Lysis Buffer	Promega
Apocynin	Sigma
Hydrogen Peroxide	Sigma
Potassium Chloride	Sigma
Disodium phosphate	Sigma
Monopotassium phosphate	Sigma

2.1.4 Table 4: Enzymes

Enzyme	**Source**
XbaI	New England Biolabs
Cre-recombinase	Miniprepped from bacterial stock in lab
BamHI	New England Biolabs

2.1.5 Table 5: Plasmids

Plasmid name/description	**Marker Gene**	**Source**
pTH460: Luciferase Reporter (Control)	*URA3*	(von der Haar *et al.*, 2017)
pTH477: Luciferase Reporter (UGAC read-through)	*URA3*	(von der Haar *et al.*, 2017)
pTH575: Luciferase Reporter (CGC → His misincorporation)	*URA3*	(von der Haar *et al.*, 2017)
pTH806: Luciferase Reporter (AGG → Lys misincorporation)	*URA3*	(von der Haar *et al.*, 2017)
pUH7	*HIS3*	(Cross, 1997)
pTH701x: pYES2 backbone	*URA3*	(Rinnerthaler *et al.*, 2012)
pTH702x: PYES2-*YNO1*	*URA3*	(Rinnerthaler *et al.*, 2012)
pTH701: pYES2 backbone	*HIS3*	(Rinnerthaler *et al.*, 2012)
pTH702: PYES2-*YNO1*	*HIS3*	(Rinnerthaler *et al.*, 2012)

2.1.6 Table 6: Strains

Organism / Strain	**Genotype(s)**
Saccharomyces cerevisiae (BY4741)	*MATa his3Δ1 leu2Δ0 met15Δ0 ura3Δ0* (wild-type) Respective *YNO1* Deletion Respective *YCK1* Deletion Respective *YCK2* Deletion Respective *HEK2* Deletion Respective *CHL1 Deletion* Respective *TIF2 Deletion*
Escherichia coli (T10)	F- *mcrA* Δ(*mrr-hsd*RMS-*mcr*BC) Φ80*lac*ZΔM15 Δ *lac*X74 *rec*A1 *ara*D139 Δ(*araleu*)7697 *gal*U *gal*K *rps*L (StrR) *end*A1 *nup*G

2.1.7 Table 7: Kits

Kits	**Source**
NucleoSpin® - Gel and PCR Clean-up	Machery-Nagel
QIAprep® Spin Miniprep Kit	Qiagen
ChargeSwitch® Plasmid Yeast Mini Kit	Fisher
Luciferase	Promega

2.2 Methods

2.2.1 Yeast Transformation

1ml of an overnight culture was harvested at room temperature in a clinical centrifuge at 5000xg, and subsequently washed first with 1ml TE then 1ml of 0.2M Lithium acetate in TE. The mix was then re-suspended in 0.1ml of 0.2M Lithium acetate in TE. 0.015ml carrier DNA (single-stranded DNA at 10mg/ml and boiled), 1µg plasmid and 0.7ml 40% PEG4000 in 0.1M Lithium acetate in TE were all added, and the mixture was vortexed and then incubated at room temperature for 1 hour on a roller. The mixture was then heat-shocked for 15 minutes at 42^0C, before being spun down in a clinical centrifuge at room temperature and 5000xg, suspended in 0.2ml sterile water, and all of it was plated on selective plates. These were left to grow at 30^0C for 48 hours.

2.2.2 E. coli Transformation

$1x10^{-3}$ ml plasmid was added to 0.1ml competent T10 *E. coli* cells and incubated for 30 minutes on ice. The mixture was then heat-shocked for 60 seconds at 42°C, placed back on ice, and 1ml LB medium was added. The mixture was then incubated for 60 minutes at 37°C, shaking. 0.1ml of this mixture was plated per LB-Amp plate (von der Haar, 2018).

2.2.3 Bacterial Miniprep

Protocol followed was from the QIAprep® Spin Miniprep Kit (QIAgen, 2015), and the cells used in this process were T10 *E. coli* cells that were previously transformed with either pTH701, pTH702, pTH460, pTH477, pTH575 or pTH806.

2.2.4 Yeast Miniprep

Protocol followed was from the ChargeSwitch® Plasmid Yeast Mini Kit (Invitrogen, 2005), and the cells used were the BY4741 *S. cerevisiae* cells having previously been transformed with pTH701 or pTH702.

Modifications added:

Fresh lyticase (2,000 U/ml in water) was used every time.

Incubation time was 4-6 hours; spheroblasts were checked visibly under microscope every ½ hr after original incubation time recommendation.

2.2.5 Marker Swap

pUH7 (Cross, 1997) was subject to restriction digest using *XbaI*. The reaction was left to incubate overnight at room temperature. Two fragments of DNA were produced, one at 3.6kb containing the *HIS3* gene, and another at 2.9kb (verified by gel electrophoresis).

Table 8: Marker Swap Restriction Digest

Component	Volume (µl)	Final Concentration
pUH7 (Cross, 1997)	10	0.1 µM
NEBuffer™ 2	3	1 unit/µl (10x stock)
XbaI	1	1 unit/µl
dH_2O	16	53% (v/v)

2.2.6 Luciferase assay

150µl of SD-HIS/URA broth, with either 2% galactose or 2% glucose, was added to each reaction to be carried out and left to grow overnight at 30^0C. One colony was added to each well. Two different strains or conditions were measured within the same assay so the relative change in fluorescence could be determined. Figure 4 shows which wells in the 96-well plate used to contain the luciferase reactions were occupied. The following morning, 30µl from each well was diluted with 120µl of fresh media and left to grow at 30^0C for 2-3 hours. The main assay consisted of transferring 30µl from each well of this culture to a corresponding well on an opaque white 96-well plate, adding 10ul of passive lysis buffer and 40ul of Dual-Glo® Reagent, incubating for 10 minutes, and then measuring the Firefly luminescence in a luminometer, as follows: 40ul of Dual-Glo® Stop & Glow® Reagent was added to each well, incubated for 10 minutes, and then Renilla luminescence was measured in a luminometer. The ratio of Firefly luminescence to Renilla luminescence was taken for all wells, and for all experimental reporter conditions this ratio was divided by the mean of the ratio for the control reporter which had the corresponding experimental conditions.

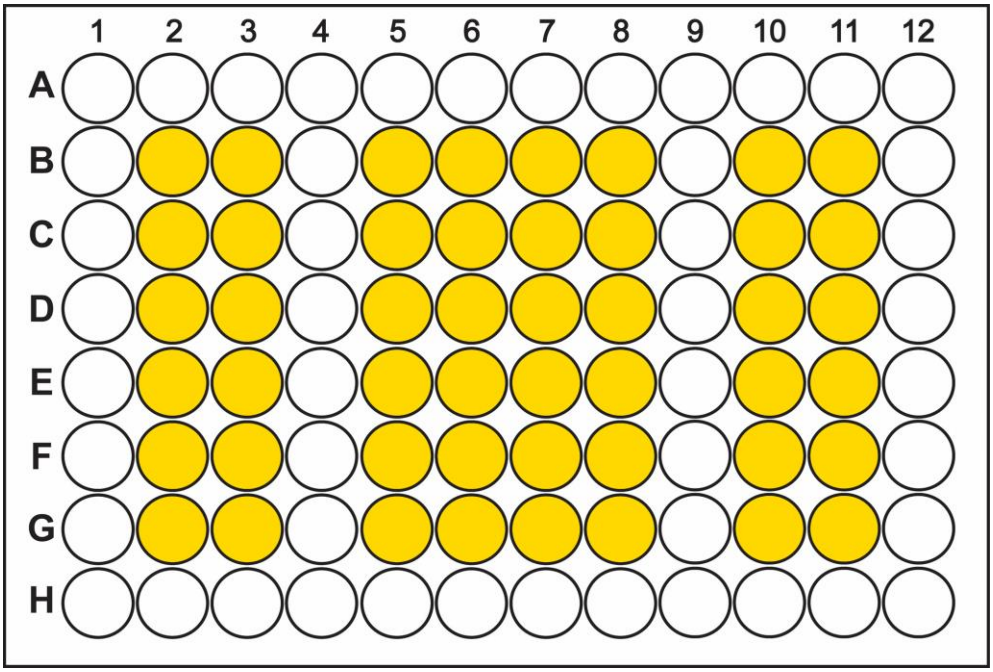

Figure 4: *Luciferase Assay Layout*

The cells populating yellow wells in each column from left to right, are as follows:
Column 1: cells of strain/condition 1 with luciferase reporter (control)
Column 2: cells of strain/condition 2 with luciferase reporter (control)
Column 3: cells of strain/condition 1 with luciferase reporter (UGAC read-through)
Column 4: cells of strain/condition 2 with luciferase reporter (UGAC-read-through)
Column 5: cells of strain/condition 1 with luciferase reporter (CGC → His misincorporation)
Column 6: cells of strain/condition 2 with luciferase reporter (CGC → His misincorporation)
Column 7: cells of strain/condition 1 with luciferase reporter (AGG → Lys misincorporation)
Column 8: cells of strain/condition 2 with luciferase reporter (AGG → Lys misincorporation)
Edited from (sittingpretty.us, 2018)

2.2.7 Growth Curves

All growth curves were conducted in transparent 24-well plates, with 1ml of media inoculated to OD_{600} 0.1 from an overnight culture in each well. The OD_{600} was measured in an optical plate reader every 30 minutes at 30°C for 24 hours. Each condition was repeated in biological triplicate.

2.2.8 5-FOA media

80ml of dH_20 and 1.6g agar was autoclaved and cooled to 50^oC. Separately, 2g glucose, 0.17g yeast nitrogen base (without amino acids or ammonium sulphate), 0.5g ammonium sulphate, 0.1g 5-FOA and 2.5ml of a 2mg/ml uracil stock were mixed and the volume adjusted to 20ml with dH_2O. The mixture was bath sonicated until the 5-FOA dissolved, and then filter sterilised into the molten agar. Glucose was then added to a final concentration of 2% (v/v), and plates were poured. These were stored at 4^0C.

2.2.9 Agarose Gel Electrophoresis

A 1% (w/v) gel was prepared using agarose and TAE, and samples were mixed with 0.5µg/mL ethidium bromide and run at 70V. The gel was disposed of in a biohazard bin and incinerated, as ethidium bromide is toxic.

2.2.10 Gel Extraction

Protocol followed was from the NucleoSpin® - Gel and PCR Clean-up manual 2 (Machery-Nagel, 2017)

2.2.11 Statistical analyses

All statistical analyses were conducted in Microsoft Excel 2016, MiniTab 18, or Python. Luciferase assay data were analysed using a two-way ANOVA with Tukey's HSD as a *post hoc*

test. Statistical significance is indicated in all figures with the following symbols: no symbol, $p < 0.05$; *, $0.05 . p < 0.01$; **, $0.01 . p < 0.001$; ***, $0.001 < p$.

2.2.12 Restriction Digest (plasmid verification)

pTH701 and pTH702 were verified after miniprep and transformation to ensure they were correct (pTH701 having one band corresponding to the length in base pairs of the whole plasmid, and pTH702 having two bands corresponding to the length in base pairs of the pYES backbone and the *YNO1* insert) and intact (pTH701 having one band, and pTH702 having two bands, in addition to any undigested plasmid bands). The reaction was left to incubate for three hours at room temperature, and then the DNA was subject to electrophoresis and following this the whole gel was viewed under UV light.

Table 9: Plasmid Verification Restriction Digest

Component	**Volume (µl)**	**Final Concentration**
Plasmid	10	0.1 µM
NEBuffer™ 2	3	1 unit/µl (10x stock)
BamHI	1	1 unit/µl
dH_2O	16	53% (v/v)

2.2.13 Hydrogen peroxide dye

Cells were grown overnight, diluted 50% (v/v) in fresh medium the next morning, and then incubated with 5µM H_2DCFDA for 2-4 hours. Samples were then spun down, washed with PBS,

diluted to OD_{600} 2 and 200µl of each sample was placed in triplicate in an opaque 96 well plate. The absolute fluorescence of each well was measured in an optical plate reader.

3 Results

3.1 Generation of Plasmids

The first experimental goal was to test the effect of overexpression of *YNO1* on three measures of fidelity – UGAC read-through, GCG → HIS misincorporation and AGG → LYS misincorporation. Both the existing *YNO1* overexpression plasmid (pTH702x) and luciferase reporters had the *URA3* marker; hence a marker swap was carried out (Cross, 1997) to replace *URA3* with *HIS3* on pTH701x and pTH702x. Cells containing this plasmid were then transformed with the *HIS3* fragment produced in the 'marker swap' reaction (2.2.5) and grown on SD-HIS media to select for successful transformants. As some cells could still contain plasmids with *URA3,* the successful transformants were streaked on plates containing 5-FOA, which selects for cells lacking the *URA3* gene. Cells that grew under these conditions therefore contained the *HIS3* selectable marker, but not the *URA3* selectable marker. Hence, the suite of reporters could now be transformed into these cells and be accurately selected for on SD-HIS/URA media.

3.2 Testing Plasmids

Before conducting measurements of translational accuracy using the luciferase plasmids, their effect on the cell (or lack thereof) needed to be determined. Cells with either pTH701 alone or with one of the four luciferase reporters were grown overnight in YPD, inoculated to OD_{600} 0.1 the following morning, and then grown for 24 hours in a plate reader. No significant difference was found in the absolute growth rates of each condition, showing that the plasmids has no effect on cellular growth (Figure 5).

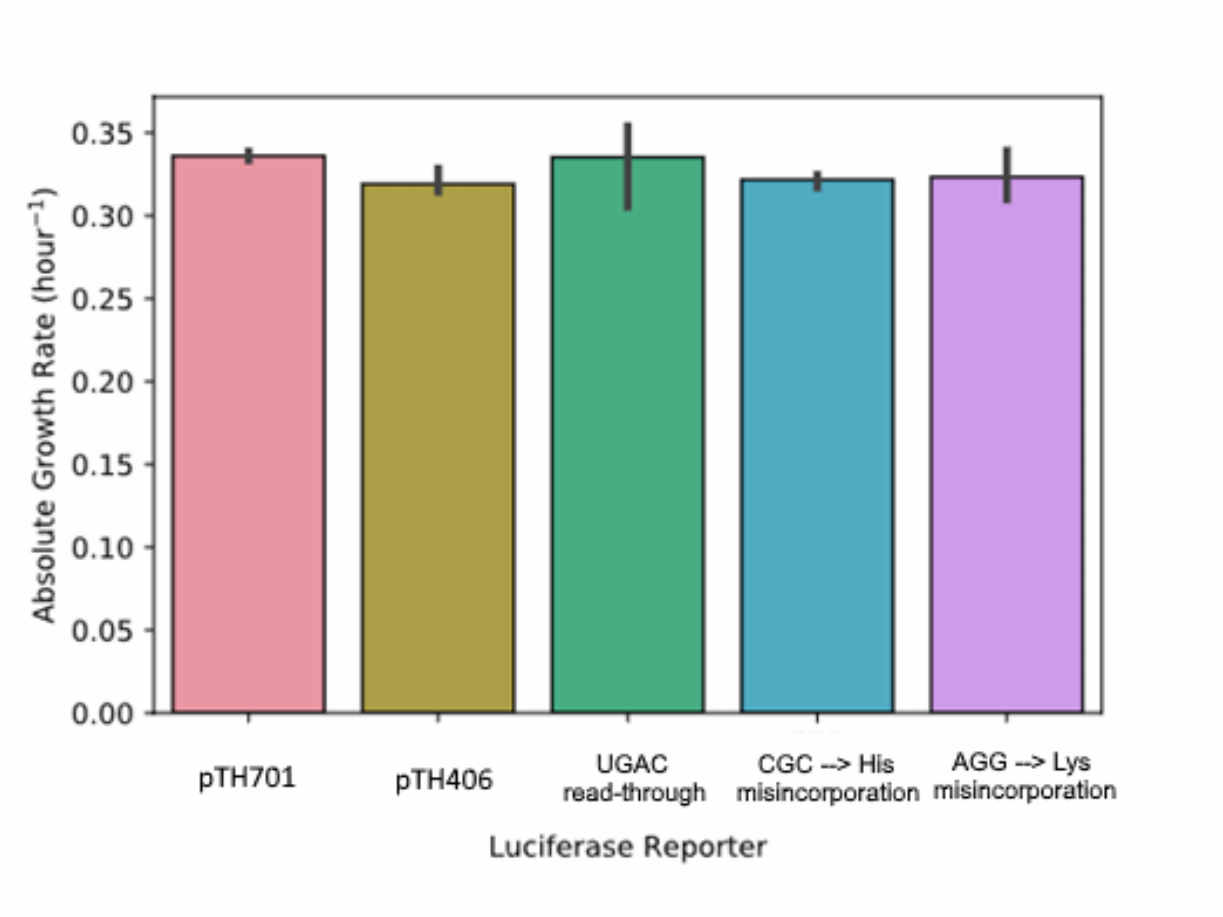

Figure 5: *The effect of luciferase reporter plasmids on absolute growth rate of wild-type strain*
Cells containing pTH701 were transformed with the suite of luciferase plasmids and grown for 24 hours in a plate reader. The absolute growth rate was determined. No significant difference was found across all conditions.
Data were analysed using a two-way ANOVA with Tukey's HSD as a post hoc test. Statistical significance is indicated with the following symbols: no symbol, $p > 0.05$; *, $p < 0.05$; **, $p < 0.01$; ***, $p < 0.001$

3.3 Overexpression of YNO1 decreases the frequency of stop-codon read-through

Cells containing a combination of one of the luciferase reporters and either the *YNO1* overexpression plasmid or control were subject to a luciferase assay. The magnitude of stop-codon read-through was subject to a highly significant decrease when *YNO1* was overexpressed relative to the wild-type, as shown in Figure 6. Amino acid misincorporation levels remained the same.

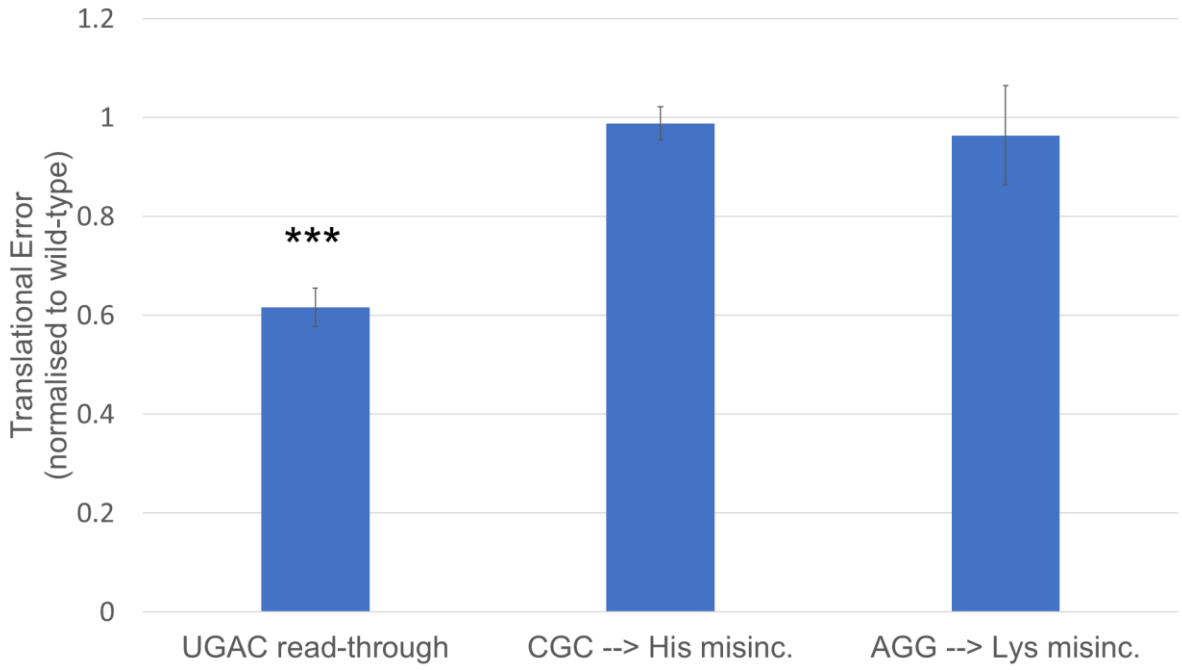

Figure 6: *Overexpression of YNO1 decreases the frequency of stop-codon read-through relative to wild-type strain*
Cells containing the suite of luciferase reporters and either a *YNO1* overexpression or control plasmid were subject to luciferase assay. The frequency of stop-codon read-through decreased significantly when *YNO1* was overexpressed.
Data were analysed using a two-way ANOVA with Tukey's HSD as a post hoc test. Statistical significance is indicated with the following symbols: no symbol, $p > 0.05$; *, $p < 0.05$; **, $p < 0.01$; ***, $p < 0.001$

3.4 Deletion of YNO1 increases the frequency of stop-codon read-through and amino acid misincorporation

Wild-type *Saccharomyces cerevisiae* cells containing pTH701 and cells with a genomic deletion of *YNO1* were subject to a luciferase assay. The *ΔYNO1* strain displayed an increased frequency of stop-codon read-through and CGC → HIS amino acid misincorporation relative to the wild-type, shown in Figure 7. In keeping with the results in 3.3, stop codon read-through appears linearly dependent on Yno1p levels.

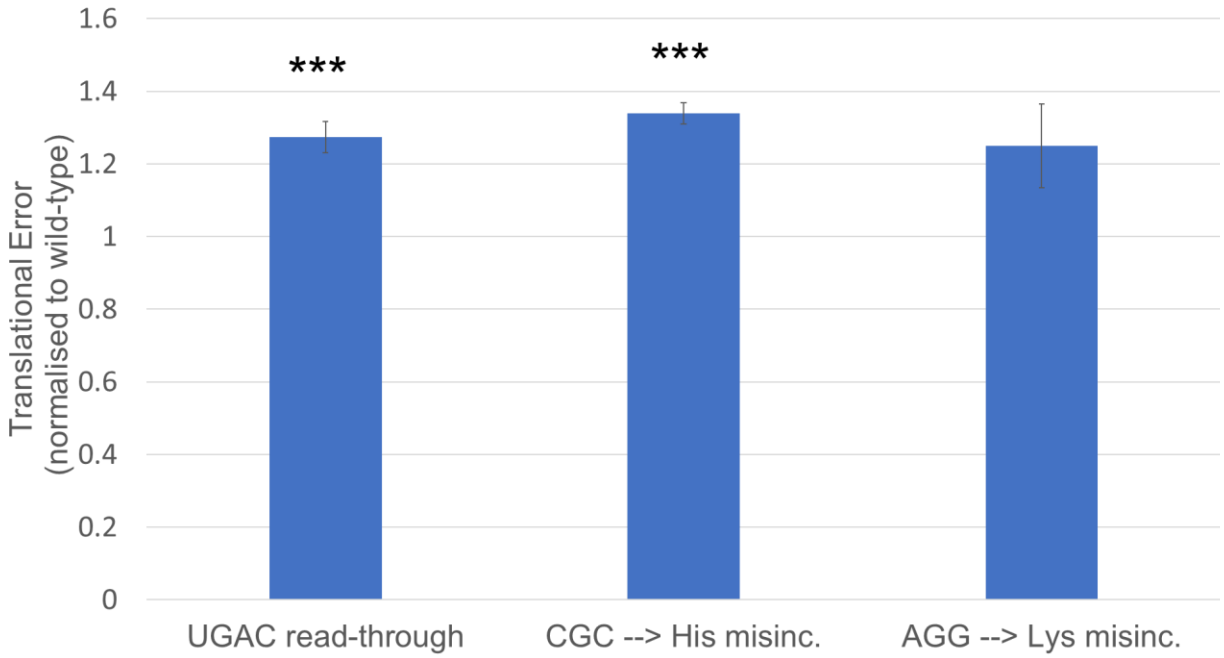

Figure 7: *Deletion of YNO1 increases the frequency of stop-codon read-through and amino acid misincorporation relative to wild-type strain*
Wild-type and *ΔYNO1* cells containing the suite of luciferase reporters were subject to luciferase assay. The frequency of stop-codon read-through and amino acid misincorporation increased significantly when *YNO1* was deleted.
Data were analysed using a two-way ANOVA with Tukey's HSD as a post hoc test. Statistical significance is indicated with the following symbols: no symbol, $p > 0.05$; *, $p < 0.05$; **, $p < 0.01$; ***, $p < 0.001$

3.5 Addition of ROS and overexpression of YNO1 exert similar influence on stop-codon read-through

As *YNO1* is responsible for production of superoxide, we hypothesised that the mechanism of stop-codon read-through observed by increased expression of *YNO1* is mediated through ROS. To test this, cells were grown overnight in selective media containing either 0.1mM or 0.25mM hydrogen peroxide, and subject to luciferase assay as normal 24 hours later. The cells incubated with 0.1mM hydrogen peroxide had a small but significant decrease in stop-codon read-through, and cells incubated with 0.25mM hydrogen peroxide had a highly significant decrease in the same reporter. Both of these mimic, albeit less strongly, the decrease in stop-codon read-through observed through overexpression of *YNO1*. These data are displayed in Figure 8, along with the data from Figure 6 and Figure 7.

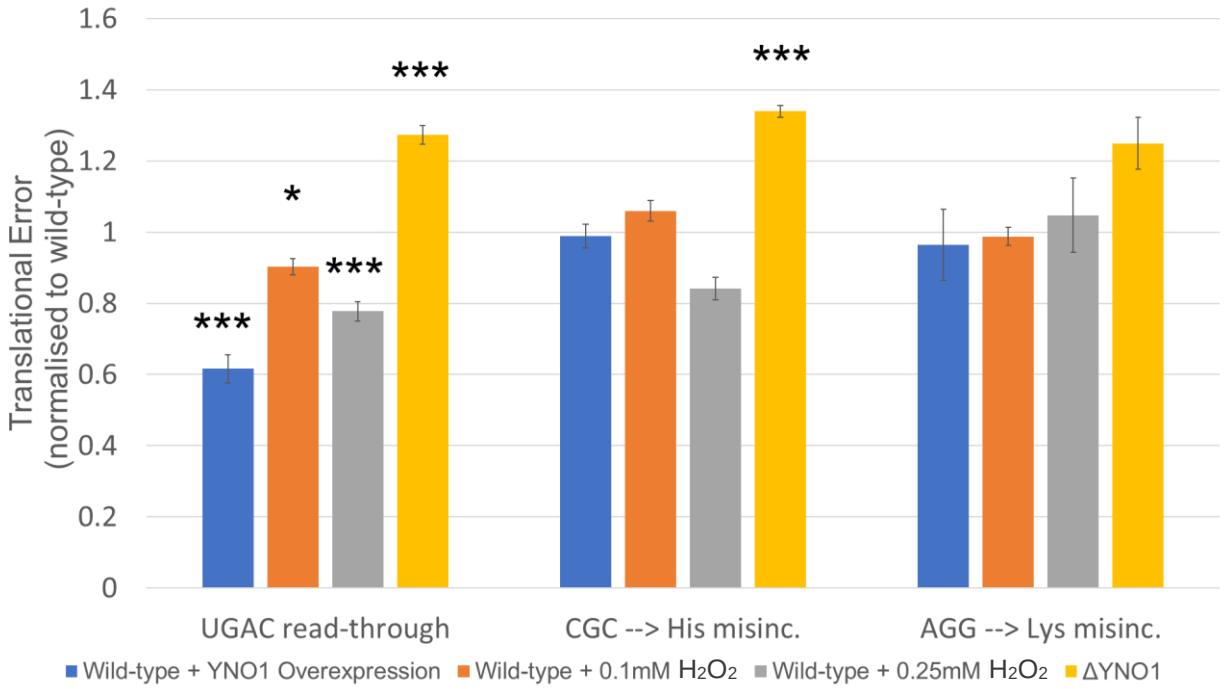

Figure 8: *Addition of hydrogen peroxide mimics the same effect on stop-codon read-through as overexpression of YNO1 does*

Cells containing the suite of luciferase reporters and either a *YNO1* overexpression or control plasmid were incubated with either 0.1mM or 0.25mM hydrogen peroxide overnight, and then subject to luciferase assay. Incubation with 0.1mM hydrogen peroxide resulted in a significant decrease in stop-codon read-through, as did incubation with 0.,25mM hydrogen peroxide, albeit with a greater magnitude. Also shown are the data from Figure 6 and Figure 7 for comparison, as they also reveal the same pattern. Overexpression of *YNO1* causes a highly significant decrease in stop-codon read-through frequency, and deletion of *YNO1* causes a highly significant increase in the same measure of infidelity.

Data were analysed using a two-way ANOVA with Tukey's HSD as a post hoc test. Statistical significance is indicated with the following symbols: no symbol, $p > 0.05$; *, $p < 0.05$; **, $p < 0.01$; ***, $p < 0.001$

3.6 Stop-codon read-through frequency is decreased through simultaneous addition of ROS and YNO1 overexpression

Data collected in 3.5 suggests a possible dose-dependent relationship between intracellular ROS levels and stop-codon read-through frequency. To test this hypothesis further, luciferase assays were carried out relative to strains other than the wild-type, namely the *YNO1* overexpression strain and the wild-type strain incubated overnight in either 0.1mM or 0.25mM hydrogen peroxide. These were subject to luciferase assays in relation to strains distinguished by varying levels of expression of *YNO1* and extracellular ROS exposure.

YNO1 overexpression and exposure to 0.25mM hydrogen peroxide, but not 0.1mM hydrogen peroxide, produced a significant improvement in stop-codon read-through relative to *YNO1* overexpression alone (Figure 9), showing that fidelity on this reporter can be improved above that which *YNO1* is capable of generating on its own.

When the wild-type strain incubated overnight in 0.1mM hydrogen peroxide was used as the baseline for comparison, stop-codon read-through was significantly increased to a similar magnitude by the overexpression strain and in the overexpression strain incubated overnight in 0.1mM hydrogen peroxide. The *ΔYNO1* strain incubated in 0.1mM hydrogen peroxide overnight displayed a relative decrease in stop-codon read-through. Lastly the wild-type strain displayed a small but significant increase in stop-codon read-through relative to this condition, indicating that a small addition of extracellular ROS improves stop-codon read-through, i.e. impairing termination (Figure 10).

Similarly, the wild-type strain incubated overnight in 0.25mM hydrogen peroxide was used as a baseline for comparison. Compared to this, the *ΔYNO1* strain incubated in 0.25mM hydrogen

peroxide displayed identical reporter outputs, showing that the levels of ROS between them either are not significantly different or something else has occurred within the cells resulting in matched fidelity. Almost identically to the pattern observed in Figure 10, relative to the baseline condition described, the wild-type displayed a highly significant increase in stop-codon read-through, whereas overexpression of *YNO1* both with and without overnight incubation in 0.25mM hydrogen peroxide resulted in a decrease in stop-codon read-through (Figure 11).

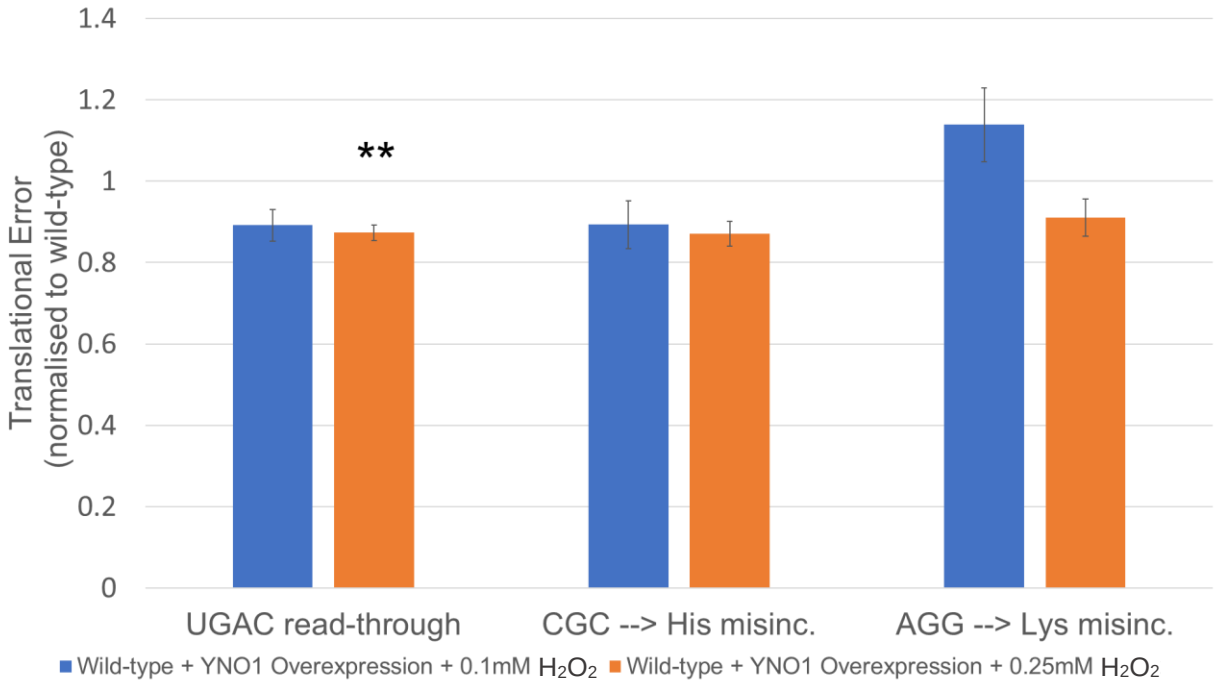

Figure 9: *Addition of hydrogen peroxide to a strain overexpressing YNO1*
Cells containing the suite of luciferase reporters and pTH702 were incubated with either 0.1mM or 0.25mM hydrogen peroxide overnight, and then subject to luciferase assay against a control that had not been incubated with hydrogen peroxide. Incubation with 0.1mM hydrogen peroxide resulted in no significant difference across any measure of infidelity. Incubation with 0.25mM hydrogen peroxide, however, resulted in a significant decrease in stop-codon read-through. Data were analysed using a two-way ANOVA with Tukey's HSD as a post hoc test. Statistical significance is indicated with the following symbols: no symbol, $p > 0.05$; *, $p < 0.05$; **, $p < 0.01$; ***, $p < 0.001$

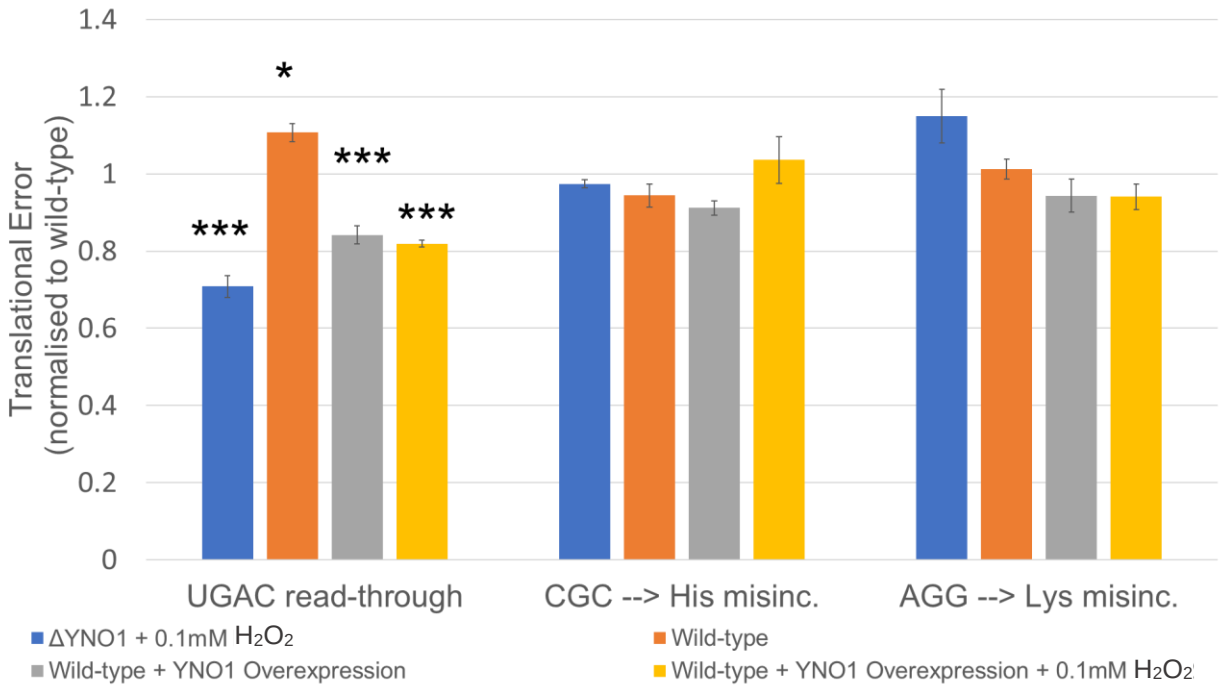

Figure 10: *Fidelity measures of various conditions relative to the wild-type strain incubated with 0.1mM hydrogen peroxide overnight*

Cells incubated with 0.1mM hydrogen peroxide overnight containing the suite of luciferase reporters were subject to luciferase assay against the wild-type strain, the wild-type strain overexpressing *YNO1*, the wild-type strain overexpressing *YNO1* and having been incubated in 0.1mM hydrogen peroxide overnight, and the *ΔYNO1* strain incubated in 0.25mM hydrogen peroxide overnight. Stop-codon read-through was significantly improved in a similar magnitude by the overexpression strain and in the overexpression strain incubated overnight in 0.1mM hydrogen peroxide. The *ΔYNO1* strain incubated in 0.1mM hydrogen peroxide overnight displayed a relative decrease in stop-codon read-through. Lastly the wild-type strain displayed a small but significant increase in stop-codon read-through relative to this condition.
Data were analysed using a two-way ANOVA with Tukey's HSD as a post hoc test. Statistical significance is indicated with the following symbols: no symbol, $p > 0.05$; *, $p < 0.05$; **, $p < 0.01$; ***, $p < 0.001$

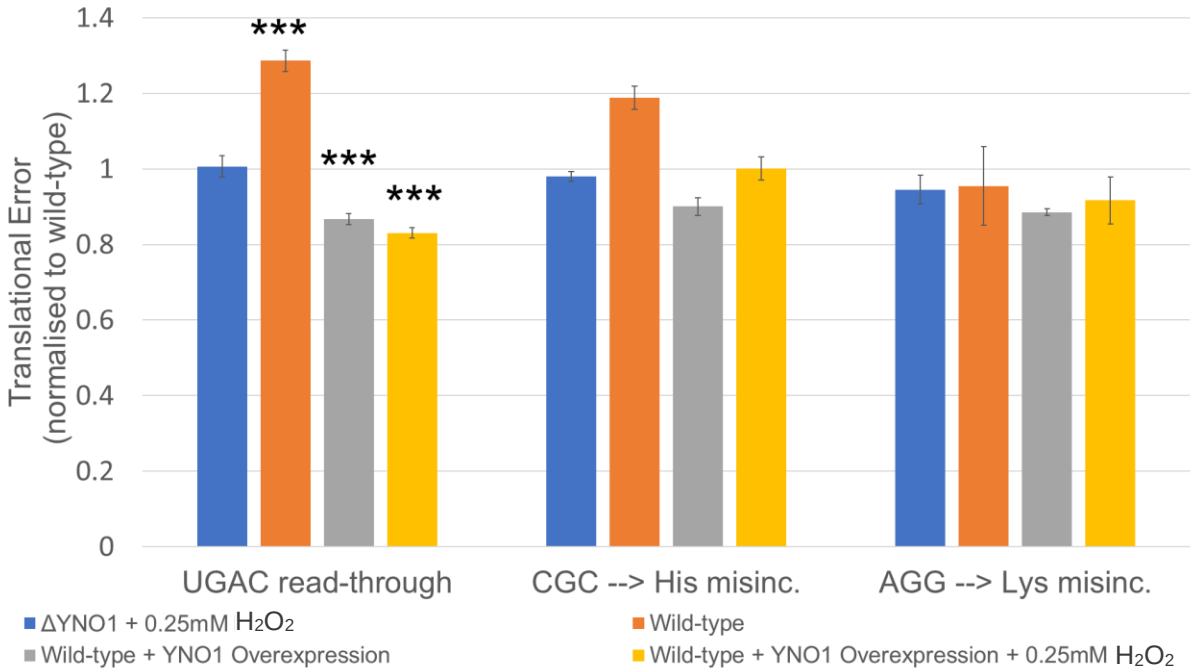

Figure 11: *Fidelity measures of various conditions relative to the wild-type strain incubated with 0.25mM hydrogen peroxide overnight*
Cells incubated with 0.25mM hydrogen peroxide overnight containing the suite of luciferase reporters were subject to luciferase assay against the wild-type strain, the wild-type strain overexpressing *YNO1*, the wild-type strain overexpressing *YNO1* and having been incubated in 0.25mM hydrogen peroxide overnight, and the *ΔYNO1* strain incubated with 0.25mM hydrogen peroxide overnight. Compared to this, the *ΔYNO1* strain incubated in 0.25mM hydrogen peroxide displayed identical reporter outputs. Relative to the baseline condition, the wild-type displayed a highly significant increase in stop-codon read-through, whereas overexpression of *YNO1* both with and without overnight incubation in 0.25mM hydrogen peroxide resulted in a decrease in stop-codon read-through.
Data were analysed using a two-way ANOVA with Tukey's HSD as a post hoc test. Statistical significance is indicated with the following symbols: no symbol, $p > 0.05$; *, $p < 0.05$; **, $p < 0.01$; ***, $p < 0.001$

3.7 YCK1, YCK2, HEK2 are all independently required for YNO1 to improve stop-codon read-through

Evidence has thus far been gathered to support the role of *YNO1*, and more broadly hydrogen peroxide, in improvement of stop-codon read-through. The manner in which it does this however

is unclear, as ROS must somehow signal to the translational machinery. Multiple genes linked through genetic interaction with *YNO1* were identified on *BioGRID* (BioGRID, 2018) and the literature (Reddi and Culotta, 2013), and strains with genomic deletions of these genes were tested in luciferase assays, containing either the control plasmid or the *YNO1* overexpression plasmids. *ΔYCK1, ΔYCK2, ΔHEK2, ΔCHL1* and *ΔTIF2* were all tested, and the results are displayed in Figure 12. The former three had no change in fidelity on any of the three reporters when *YNO1* was overexpressed, whereas the latter two mimicked the usual decrease in stop-codon read-through when *YNO1* was overexpressed. Deletion of *YCK1*, *YCK2* and *HEK2* abrogated the fidelity improvement, therefore showing that their presence is independently required for *YNO1* to improve stop-codon read-through.

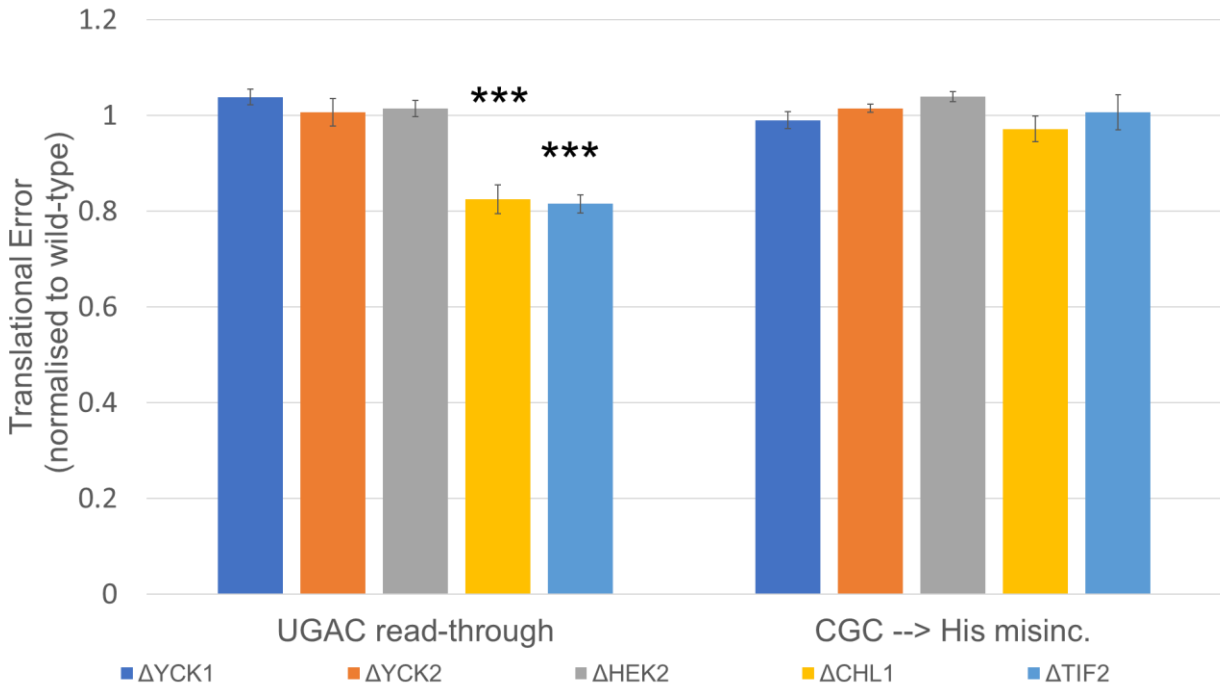

Figure 12: *Translational fidelity of ΔYCK1, ΔYCK2, ΔHEK2, ΔCHL1 and ΔTIF2 all overexpressing YNO1 relative to these strains not overexpressing YNO1*
ΔYCK1, ΔYCK2, ΔHEK2, ΔCHL1 and ΔTIF2 with and without a *YNO1* overexpression plasmid were all subject to luciferase assay. The former three had no change in fidelity on any of the three reporters when *YNO1* was overexpressed, whereas the latter two mimicked the usual

decrease in stop-codon read-through when *YNO1* was overexpressed. Deletion of YCK1, YCK2 and HEK2 abrogated the fidelity improvement.
Data were analysed using a two-way ANOVA with Tukey's HSD as a post hoc test. Statistical significance is indicated with the following symbols: no symbol, $p > 0.05$; *, $p < 0.05$; **, $p < 0.01$; ***, $p < 0.001$

3.8 ROS improves fidelity in ΔYCK1 strain

In order to elucidate if the hypothesized signalling pathway from superoxide produced by Yno1p to the translational machinery is different to the influence of ROS exposure on fidelity, the *ΔYCK1* strain was incubated in 0.1mM and 0.25mM hydrogen peroxide overnight and subject to a luciferase assay relative to the *ΔYCK1* on its own. Both exposure to 0.1mM and 0.25mM hydrogen peroxide resulted in a highly significant decrease in stop-codon read-through, and exposure to 0.25mM hydrogen peroxide also significantly decreased amino acid misincorporation. This shows that, despite YCK1 being required for fidelity improvement mediated by Yno1p as shown in 3.7, it is not required for fidelity improvement mediated by simple ROS exposure.

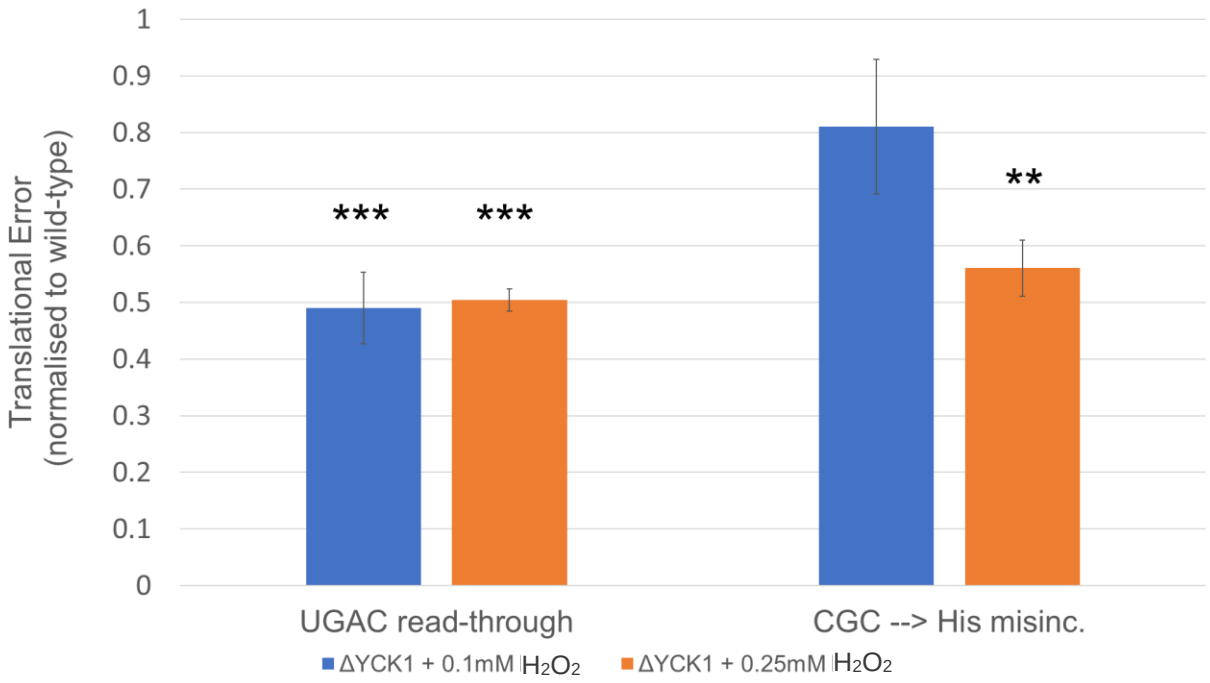

Figure 13: *Addition of hydrogen peroxide improves translational fidelity in a ΔYCK1*
A *ΔYCK1* strain was incubated in either 0.1mM or 0.25mM hydrogen peroxide overnight and subject to a luciferase assay relative to the *ΔYCK1* on its own. Both exposure to 0.1mM and 0.25mM hydrogen peroxide resulted in a highly significant improvement in stop-codon read-through, and exposure to 0.25mM hydrogen peroxide also significantly improved amino acid misincorporation.
Data were analysed using a two-way ANOVA with Tukey's HSD as a post hoc test. Statistical significance is indicated with the following symbols: no symbol, $p > 0.05$; *, $p < 0.05$; **, $p < 0.01$; ***, $p < 0.001$

3.9 Nourseothricin (NTC) decreases absolute growth rate

As *YNO1* was found to exert a profound influence on translational fidelity, the question of whether it improves or worsens sensitivity to error-inducing drugs was investigated. The drug of choice was nourseothricin (NTC), a compound known to decrease translational fidelity (Sigma, 2019). Cells were grown overnight in SD-HIS/URA media, inoculated to OD_{600} 0.1 the following

morning, and NTC was added at 2µg/ml, 4µg/ml and 8µg/ml. They were then grown for 24 hours in a plate reader at 30^0C. The absolute growth rates were determined.

NTC significantly decreased the absolute growth rate at 2µg/ml compared to the wild-type, then significantly decreased it again relative to the growth rate at 2µg/ml when 4µg/ml was added. 8µg/ml had the same effect as 4µg/ml, where the cells grew at a minute proportion of the speed at which they normally grow without the presence of NTC. Hence translational fidelity is a key regulator of absolute growth rate, with the cells being able to tolerate a relatively small amount of infidelity (2µg/ml) but suffer immensely under higher concentrations of NTC. These results are displayed in Figure 14.

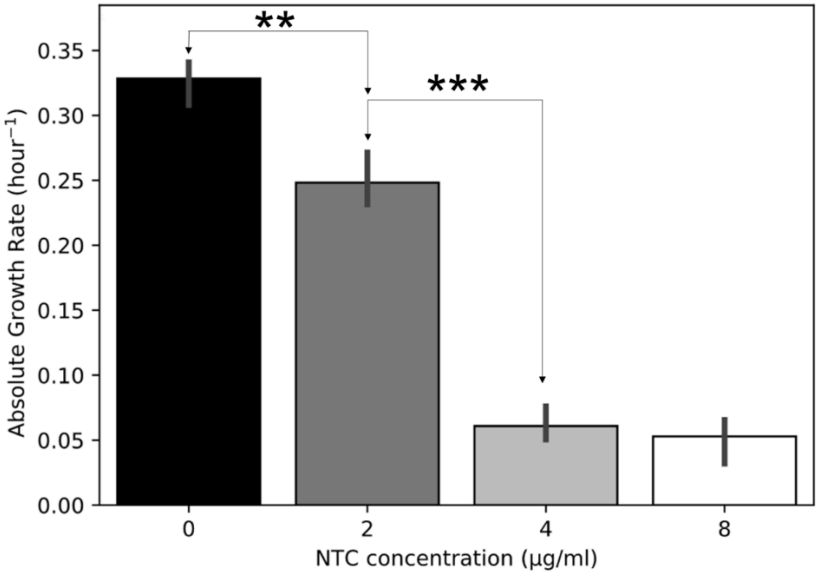

Figure 14: *The effect of nourseothricin (NTC) on the absolute growth rate of the wild-type strain* NTC significantly decreases the absolute growth rate of the wild-type strain at 2µg/ml, then significantly decreases it again relative to the growth rate at 2µg/ml when 4µg/ml is added. 8µg/ml has the same effect as 4µg/ml, where the cells barely grow at all. Significance markings in graph are the most pertinent interpretations of this set of data to the overall thesis conclusion. Data were analysed using a two-way ANOVA with Tukey's HSD as a post hoc test. Statistical significance is indicated with the following symbols: no symbol, $p > 0.05$; *, $p < 0.05$; **, $p < 0.01$; ***, $p < 0.001$

3.10 Overexpression of YNO1 increases sensitivity to error-inducing drugs

The absolute growth rate of the wild-type compared to the *YNO1* overexpression strain was determined, as well as the effect of NTC on both, with results displayed in Figure 15. Cells were grown overnight in SD-HIS/URA media, inoculated to OD6000.1 the following morning, and NTC was added at 2µg/ml, 4µg/ml and 8µg/ml. They were then grown for 24 hours in a plate reader. The absolute growth rates were determined. Without NTC, both strains had the same absolute growth rate, showing that *YNO1* overexpression had no effect on cellular growth. NTC at 4µg/ml and 8µg/ml had the same effect on both strains, severely capping the absolute growth rate. Of note is the different response to 2µg/ml NTC, with there being a significant difference in growth rate at this concentration. The *YNO1* overexpression strain grew slower at this concentration, showing that *YNO1* increases the sensitivity to error-inducing drugs. Despite improving fidelity, as shown in 3.3, *YNO1* influences the cell to grow slower under error-prone conditions.

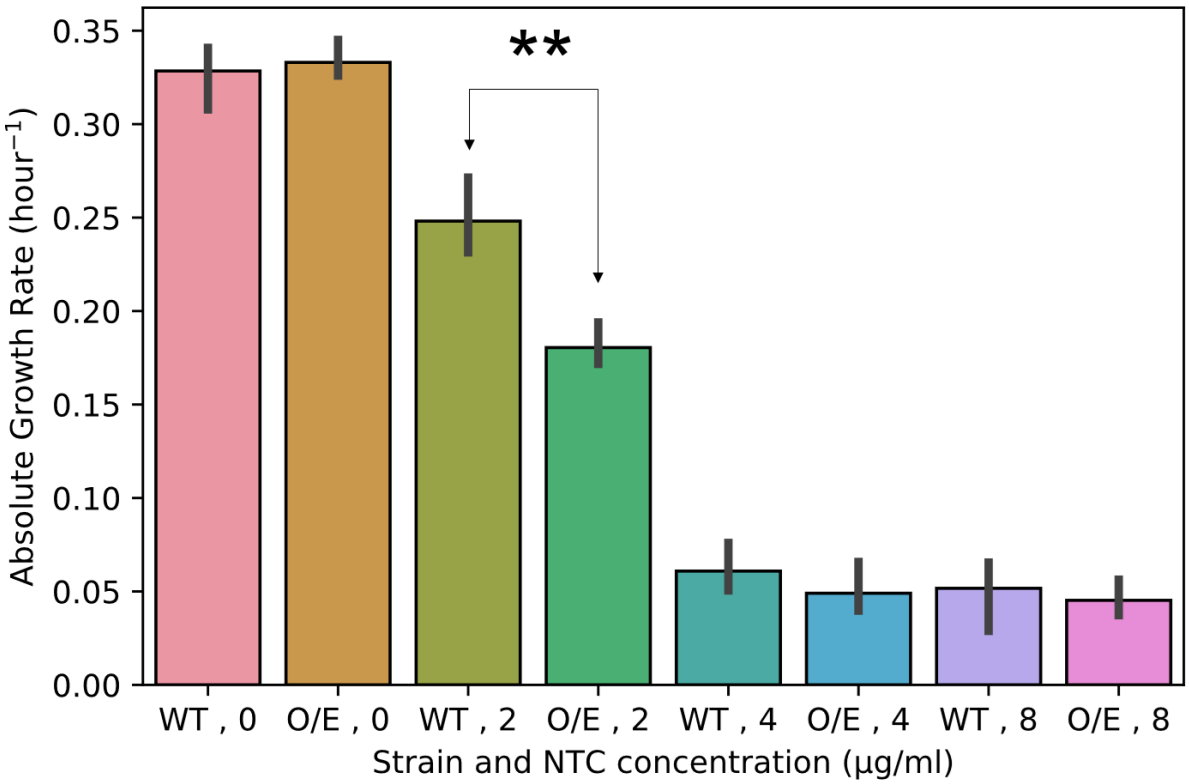

Figure 15: *The absolute growth rate of the wild-type strain compared to the YNO1-overexpression strain exposed to different concentrations of NTC*
Without NTC, both strains have the same absolute growth rate, showing that *YNO1* overexpression has no effect on cellular growth. NTC at 4µg/ml and 8µg/ml had the same effect on both strains, severely capping the absolute growth rate. Growth rate was significantly different at 2µg/ml NTC. The *YNO1* overexpression strain grew slower at this concentration.
X-axis legend:
WT: wild-type strain
O/E: *YNO1* overexpression strain
Numbers: Concentration of NTC corresponding to that bar
Significance markings in graph are the most pertinent interpretations of this set of data to the overall thesis conclusion.
Data were analysed using a two-way ANOVA with Tukey's HSD as a post hoc test. Statistical significance is indicated with the following symbols: no symbol, $p > 0.05$; *, $p < 0.05$; **, $p < 0.01$; ***, $p < 0.001$

3.11 Deletion of YNO1 does not augment sensitivity to error-inducing drugs

Similarly, the absolute growth rate at varying concentrations of NTC of the *ΔYNO1* strain was determined and compared to the wild-type strain, and results are displayed in Figure 16. Cells were grown overnight in SD-HIS/URA media, inoculated to OD_{600} 0.1 the following morning, and NTC was added at 2µg/ml, 4µg/ml and 8µg/ml. They were then grown for 24 hours in a plate reader at 30^0C, and the absolute growth rates determined. Both grew with identical maximum rates at each concentration of NTC, with 2µg/ml significantly decreasing the growth rate, and 4µg/ml and 8µg/ml significantly decreasing it by the same magnitude. In contrast to the effect of overexpression of *YNO1*, both the wild-type and *ΔYNO1* strains grew equally as fast at 2µg/ml, whereas as found in section 3.10, overexpression of *YNO1* increases the sensitivity to NTC at this concentration. This shows that deletion and overexpression of *YNO1* do not have an equal and opposite effect on sensitivity to error-inducing drugs, as one might have hypothesised.

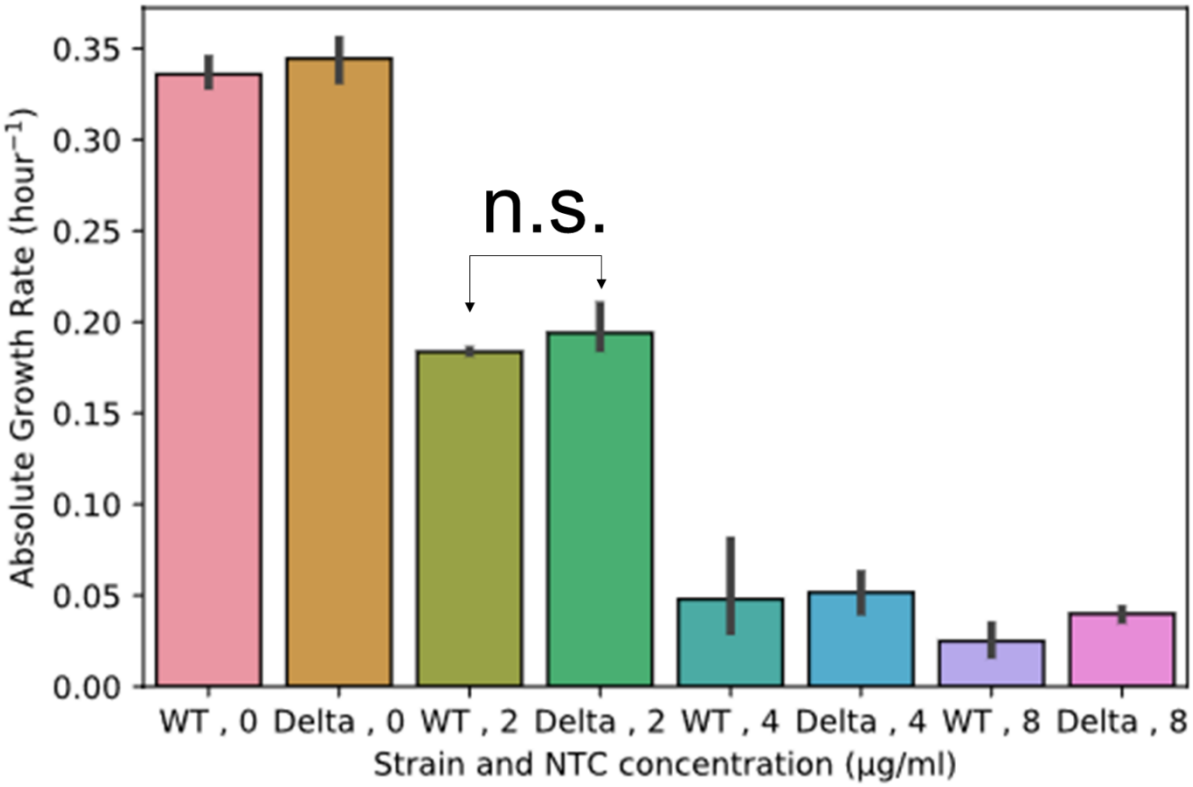

Figure 16: *The absolute growth rate of the wild-type strain compared to the ΔYNO1 strain exposed to different concentrations of NTC*

Both strains grew with identical maximum rates at each concentration of NTC, with 2µg/ml significantly decreasing the growth rate, and 4µg/ml and 8µg/ml significantly decreasing it by the same magnitude. Both the wild-type and *ΔYNO1* strains grew equally as fast at 2µg/ml.

X-axis legend:

WT: wild-type strain

Delta: *ΔYNO1* strain

Numbers: Concentration of NTC corresponding to that bar

Significance markings in graph are the most pertinent interpretations of this set of data to the overall thesis conclusion.

Data were analysed using a two-way ANOVA with Tukey's HSD as a post hoc test. Statistical significance is indicated with the following symbols: no symbol, $p > 0.05$; *, $p < 0.05$; **, $p < 0.01$; ***, $p < 0.001$

3.12 ROS addition has a similar effect on NTC sensitivity as overexpression of YNO1

In the same vain as was conducted using luciferase assays, the absolute growth rate of the wild-type exposed to 0.1mM hydrogen peroxide and varying concentrations of NTC was determined. . Cells were grown overnight in SD-HIS/URA media, inoculated to OD_{600} 0.1 the following morning, and NTC was added at 2µg/ml, 4µg/ml and 8µg/ml. They were then grown for 24 hours in a plate reader. The absolute growth rates were determined, and displayed in Figure 17. The hydrogen peroxide was added at the same time as the NTC. 0.1mM hydrogen peroxide has no effect on absolute growth rate in the wild-type strain, growing with equal maximum rates at every level of NTC concentration tested. However at 4µg/ml and 8µg/ml, the wild-type strain grew equally as fast, as previously shown in Figure 14, but the wild-type strain incubated with 0.1mM hydrogen peroxide had a significantly lower absolute growth rate at 8µg/ml than at 4µg/ml. This shows that 0.1mM hydrogen peroxide increases sensitivity to errors under this magnitude of error-prone conditions. This mimics what *YNO1* overexpression does, albeit at a higher concentration of NTC.

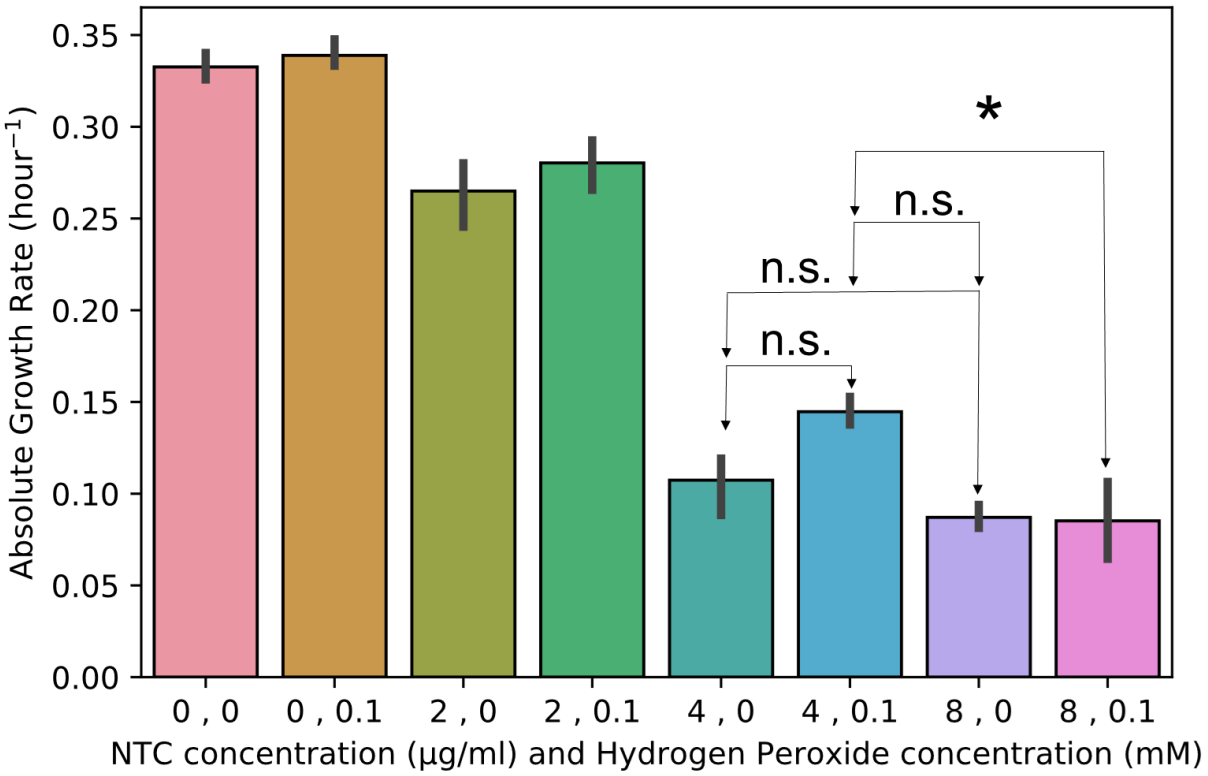

Figure 17: *The absolute growth rate of the wild-type strain compared to the wild-type strain incubated in 0.1mM hydrogen peroxide overnight exposed to different concentrations of NTC*
0.1mM hydrogen peroxide has no effect on absolute growth rate in the wild-type strain, growing with equal maximum rates at every level of NTC concentration tested. At 4µg/ml and 8µg/ml, the wild-type strain grew equally as fast, but the wild-type strain incubated with 0.1mM hydrogen peroxide had a significantly lower absolute growth rate at 8µg/ml than at 4µg/ml.
X-axis legend:
First number: NTC concentration
Second number: hydrogen peroxide concentration
Numbers: Concentration of NTC corresponding to that bar
Significance markings in graph are the most pertinent interpretations of this set of data to the overall thesis conclusion.
Data were analysed using a two-way ANOVA with Tukey's HSD as a post hoc test. Statistical significance is indicated with the following symbols: no symbol, $p > 0.05$; *, $p < 0.05$; **, $p < 0.01$; ***, $p < 0.001$

3.13 Apocynin is not a YNO1-specific inhibitor

YNO1 has so far been demonstrated to exert a significant effect on translational fidelity as well as on cellular sensitivity to error-inducing drugs. Both domains of influence can be mimicked with a small addition of ROS, suggesting that the mechanism by which *YNO1* exerts its effect on these properties is linked to the superoxide it catalyses production of. This is not self-evident though; overexpressing *YNO1* definitely leads to an increase in the copy number of *YNO1* in the cell, but does not necessarily increase the frequency of Yno1p-catalysed reactions as the latter has not directly been initiated experimentally. In order to confirm if the catalytic activity of Yno1p is what is causing the observed effects, the active site of Yno1p should be disrupted and the experiments repeated; if the same effect is observed, then it is exclusively the copy number of *YNO1* which is having an effect, whereas if the effect is abrogated then the catalysis of NADPH is the key component to the influence it exerts.

There are no known inhibitors of Yno1p in yeast. However, apocynin is an inhibitor of human NOX enzymes (Kim *et al.*, 2012). There is no published data on the effect of this compound in *Saccharomyces cerevisiae* at the current time, so this was determined. Its effect on absolute growth rate was measured by growing wild-type and *ΔYNO1* strains overnight in YPD, inoculating to OD_{600} 0.1 the following morning, and adding varying concentrations of apocynin: 100µM, 200µM and 500µM (previous work in the lab determined these to be standard working concentrations for yeast) (Figure 18).

The wild-type strain grew with identical absolute growth rates across all concentrations of apocynin tested. In contrast, the *ΔYNO1* strain experienced a significant decrease in absolute growth rate between 100µM and 200µM. This proves that apocynin has an effect on *ΔYNO1* strain, but not the wild-type strain. As such, apocynin is therefore not a specific inhibitor of

Yno1p as it exerts an effect in the absence of *YNO1*. Hence, Yno1p cannot be inhibited using apocynin for use in this thesis. Alternative inhibition mechanisms could have been tested, as mentioned in the discussion section, though due to the time constraints they were not pursued.

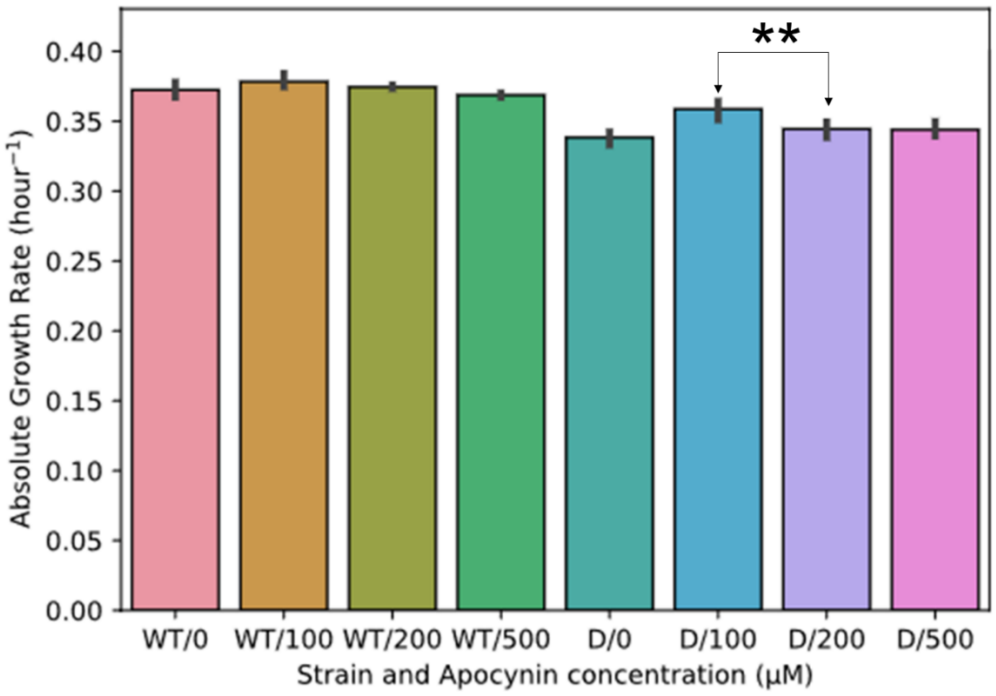

Figure 18: *The absolute growth rate of the wild-type strain compared to the ΔYNO1 strain exposed to different concentrations of apocynin*
The wild-type strain grew with identical absolute growth rates across all concentrations of apocynin tested. In contrast, the *ΔYNO1* strain experienced a significant decrease in absolute growth rate between 100µM and 200µM.
X-axis legend:
WT: Wild-type strain
D: *ΔYNO1* strain
Number: Apocynin concentration
Numbers: Concentration of NTC corresponding to that bar
Significance markings in graph are the most pertinent interpretations of this set of data to the overall thesis conclusion.
Data were analysed using a two-way ANOVA with Tukey's HSD as a post hoc test. Statistical significance is indicated with the following symbols: no symbol, $p > 0.05$; *, $p < 0.05$; **, $p < 0.01$; ***, $p < 0.001$

3.14 Hierarchy of intracellular ROS levels across wild-type, YNO1 overexpression and YNO1 deletion strains

The effect of *YNO1* on translational fidelity and cellular sensitivity to error-inducing drugs was demonstrated to be mimicked by a small addition of hydrogen peroxide (section 3.5). The translational fidelity data showed a clear additive effect – higher levels of hydrogen peroxide added and *YNO1* expression correlated with a decrease in stop-codon read-through. However, it is not clear how the intracellular levels of ROS compare between different strains. Once determined, a pattern can be searched for: is there a clear positive correlation between intracellular ROS levels and improvement in stop-codon read-through?

To measure intracellular ROS levels, 5µM H_2DCFDA was used as a stain and the cells were treated in the manner described in 2.2.13. The fluorescence for the stained cells was displayed as a fold change over the same conditions without the stain (Figure 19).

The wild-type and *ΔYNO1* strains displayed the same intracellular ROS levels, implying that the cell adapts to having no *YNO1* expressed in the cell and the ROS levels are maintained by some other compensatory means. The *ΔYNO1* strain with the *YNO1* overexpression plasmid displayed a higher level of intracellular ROS than these two conditions alone described, and the wild-type strain containing the *YNO1* overexpression plasmid displayed a highly significant level over this. From the lowest level of intracellular ROS to the highest, therefore, is as follows: wild-type and *ΔYNO1* (the same), *ΔYNO1* strain with the *YNO1* overexpression plasmid, and finally the wild-type strain containing the *YNO1* overexpression plasmid. Though taken as self-evident before due to previous work done using YNO1, these data are consistent with overexpression of *YNO1* increasing the level of ROS within the cell.

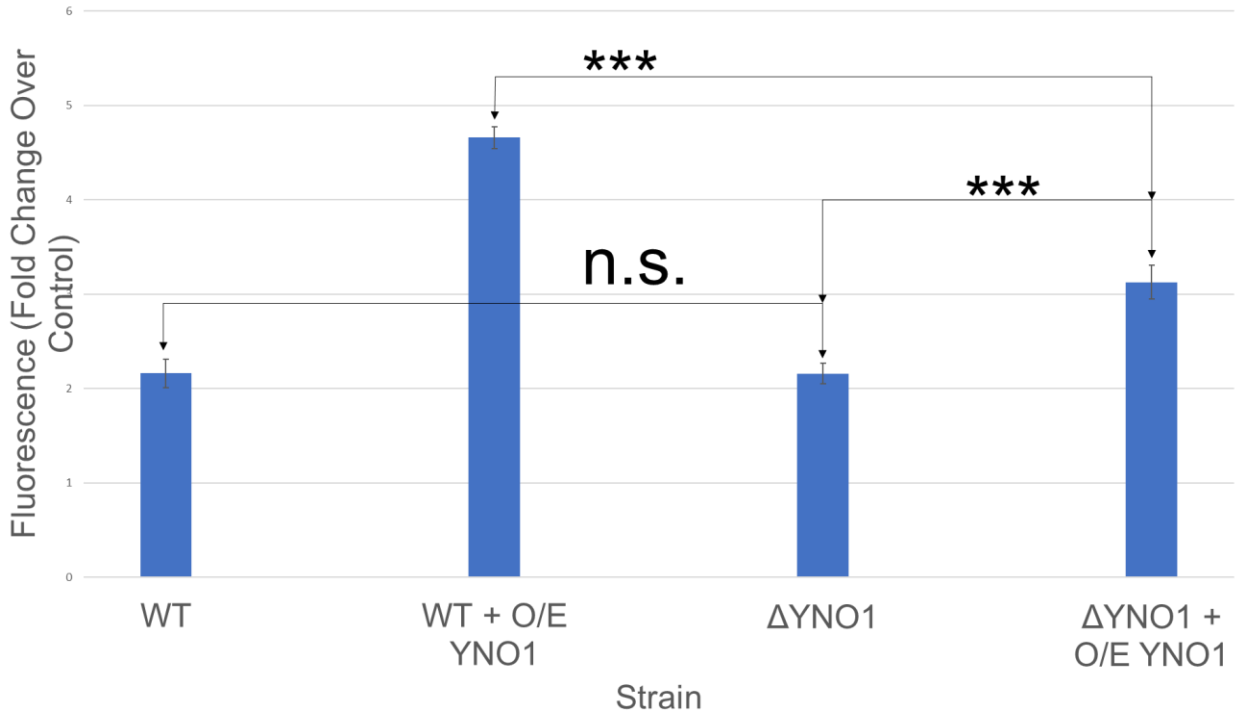

Figure 19: *Relative intraceullar ROS levels measured via fluorescence emitted from prior incubation with H_2DCFDA between the wild-type strain, YNO1-overexpression strain, ΔYNO1 strain and ΔYNO1 strain overexpressing YNO1*
The wild-type and *ΔYNO1* strains displayed the same intracellular ROS levels. The *ΔYNO1* strain with the *YNO1* overexpression plasmid displayed a highly significantly greater level of intracellular ROS than the previous two described, and the wild-type strain containing the *YNO1* overexpression plasmid displayed a highly significant level over this.
X-axis legend:
WT: wild-type strain
WT + O/E *YNO1*: wild-type strain with *YNO1* overexpression plasmid
Δ*YNO1: ΔYNO1* strain
Δ*YNO1* + O/E *YNO1*: *ΔYNO1* strain with *YNO1* overexpression plasmid
Significance markings in graph are the most pertinent interpretations of this set of data to the overall thesis conclusion.
Data were analysed using a two-way ANOVA with Tukey's HSD as a post hoc test. Statistical significance is indicated with the following symbols: no symbol, $p > 0.05$; *, $p < 0.05$; **, $p < 0.01$; ***, $p < 0.001$

4 Discussion

4.1 The mutual relationship between ageing and translational fidelity

The control of translational fidelity is an important parameter in maintaining healthy ageing in yeast (von der Haar *et al.*, 2017). Since the 1960s, the relationship between accuracy and ageing has been debated at length (Orgel, 1970), but the specific nature of their link is still unknown. One hypothesis is that the error rate is affected by ageing, possibly caused by a decreased volume of translational activity in ageing cells (Conn and Qian, 2013), but the relationship between translational output, speed and infidelity is not uniform and is subject to high variability (von der Haar *et al.*, 2017). The alternative hypothesis is that ageing is affected by changes in fidelity; for example, if an organism has high levels of infidelity, does it live longer? Again, the literature varies in its conclusions, with some studies reporting positive correlations between translational fidelity level and longevity (Azpurua *et al.*, 2013) and other report the opposite effect (Schosserer *et al.*, 2015; von der Haar *et al.*, 2017). However, the general pattern here is that evolution has coupled the lifespan of an organism positively with high levels of translational fidelity (Ke *et al.*, 2017), and that very high levels of infidelity are incompatible with healthy ageing (von der Haar *et al.*, 2017). What remains a stable conclusion across the literature, however, is that error rates remain constant across organisms and tissues of different ages (Harley *et al.*, 1980; Stahl *et al.*, 2004).

4.2 The role of YNO1 in regulating translational fidelity

4.2.1 The effect of YNO1 on translational fidelity

YNO1 was identified in this study as an important regulator of translational fidelity. When overexpressed, it decreased the frequency of stop-codon read-through. When deleted, the frequency of stop-codon read-through and one measure of amino acid misincorporation increases. Stop-codon read-through in particular is clearly dependent on Yno1p levels.

4.2.2 The role of ROS in the effect of YNO1 on translational fidelity

The mechanism by which Yno1p signals to regulate frequency of stop-codon read-through is not clear. Addition of hydrogen peroxide at 0.1mM and 0.25mM overall mimicked the same effect *YNO1* had on fidelity, implying that the superoxide produced by Yno1p is the mediator of this change. The reaction Yno1p catalyses is known to produce superoxide, which is delivered to SOD1, and then this is known to have an effect on glucose repression (Reddi and Culotta, 2013), but the hypothesis here could be that SOD1 also converts the superoxide to peroxide and then this signals to the translational machinery. The findings here run counter to the previous presumption that ROS is universally a detriment to translational fidelity; for example, ROS accumulate and oxidise tRNAs, causing mistranslation (Mohler and Ibba, 2017).

The resolution to these conflicting findings could be that the peroxide added to the cells, and the superoxide produced by Yno1p, both upregulate fidelity indirectly, but instead through upregulating the cellular stress response. However, the current evidence from the literature seems to promote the opposite conclusion – that stop-codon read-through being impaired

increases the stress response, not that the stress response improves stop-codon read-through (Katz *et al.*, 2016). As this area is still nascent, there is still place for this hypothesis to be investigated in the context of our experimental results.

Another potential resolution is that *Saccharomyces cerevisiae* simply adapts to the level of ROS within the cell, and that modulated translational fidelity is one of the ways this adaptation manifests itself. It is known that *Saccharomyces cerevisiae* incubated in 0.2mM hydrogen peroxide, a very similar concentration to the ones tested here, result in a significant increase in stop-codon read-through (Gerashchenko, Lobanov and Gladyshev, 2012). However, the difference between those experiments and the ones conducted here is that the peroxide was only added for 5 or 30 minutes. Cells were incubated here for a full 24 hours in hydrogen peroxide. Hence it is reasonable to hypothesize that ROS exposure of a certain threshold causes a short-term decrease in fidelity as the translational machinery is impaired, but that the cell overall decreases the level of fidelity to compensate for this. It would be interesting to observe a general increase in other measures of fidelity using different luciferase reporters, as their permanent increase under high-ROS conditions would potentially be compensated for by a decreased level of stop-codon read-through. During ageing, the cell produces more ROS through YNO1, but the cell adapts to this, overall maintaining fidelity levels. This idea is further supported by the observation that fidelity can be improved even further by combining hydrogen peroxide exposure and *YNO1* overexpression – or simply, the more oxidative stress, the greater the cell needs to modulate certain measures of fidelity to maintain overall fidelity. However, when 0.1mM hydrogen peroxide was added to a strain overexpressing *YNO1*, no improvement in fidelity was found, showing that there is a limit to this ROS/*YNO1*-mediated fidelity improvement pathway.

The relationship between ROS and *YNO1* is further complicated by multiple observations made in this study. The first is that deletion of genomic *YNO1* increases frequency of stop-codon read-through, as well as amino acid misincorporation, relative to the wild-type. However, the levels of ROS in the wild-type and *ΔYNO1* strain are the same. Hence, there is not a linear relationship between global ROS production and translational fidelity.

The second complication is that *YCK1* was identified as necessary for mediating the signal between Yno1p and stop-codon read-through. When hydrogen peroxide was added to a Δ*YCK1* strain, stop-codon read-through and amino acid misincorporation both improved significantly. Hence, ROS is able to improve fidelity in the absence of the Yno1p pathway, meaning ROS and Yno1p exert their similar effect on fidelity through independent mechanisms that are nonetheless able to influence fidelity in an additive manner.

Both of these interesting observations currently do not have an explanation, but instead open up a new area of investigation.

4.2.3 Downstream signalling molecules from YNO1 to the ribosome

Three genes were identified as being independently necessary for *YNO1* to influence translational fidelity – *YCK1, YCK2, and HEK2*. The previous two are paralogs, and were previously identified as downstream signalling players from Yno1p in its influence on glucose repression (Reddi and Culotta, 2013). In this pathway, Yno1p produces superoxide, which signals to SOD1 to bind to a C-terminal degron on YCK1 and YCK2 and stabilise both kinases through production of hydrogen peroxide. Could a second role of this pathway be to influence

translational fidelity? YCK1 is currently only directly linked to translation in one context: it activates translation of ASH1 mRNA (Paquin *et al.*, 2007). There is no known link between ASH1 and fidelity, ageing or anything else covered in this thesis, so this discovery opens up a new area of investigation – in what manner does YCK1, YCK2 and HEK2 regulate fidelity?

The connection between *YNO1* and *HEK2* is completely unknown. In isolation, HEK2 is implicated in maintenance of telomeres; telomere length is correlated strongly with lifespan, highlighting an even greater spotlight on this gene as a potential link between *YNO1,* translational fidelity and ageing (Denisenko and Bomsztyk, 2002).

YCK1 and YCK2 are paralogs, so should have similar functions, but both are required independently for *YNO1* to influence fidelity. Alternatively, perhaps a threshold total amount of these proteins is needed to exert an effect, and deletion of one of them lowers the level beneath this threshold?

4.2.4 The effect of YNO1 on sensitivity to error-inducing drugs

YNO1 was investigated as a potential regulator of sensitivity to error-inducing drugs, namely nourseothricin (NTC). NTC induces miscoding through an unknown mechanism (Kochupurakkal and Iglehart, 2013), and in this study it was observed to decrease absolute growth rate in a dose-dependent manner. When *YNO1* was overexpressed, the sensitivity of the cells to NTC increased. When combined with the luciferase data, *YNO1* improves fidelity, but makes the cell more sensitive to error-inducing drugs. In the absence of a mechanism of action for NTC, this

combination of results appears counter-intuitive – how can *YNO1* simultaneously make the translational machinery more and less robust against errors? Regardless, it's possible that the ROS produced by Yno1p causes sufficient oxidative stress to decrease the fidelity of certain parts of the translational machinery, and these same targets are subject to influence by NTC too, so overall they influence fidelity in an additive manner. In another interesting observation, deletion of *YNO1* doesn't decrease sensitivity to NTC, as one might predict from the data just described. The wild-type and *ΔYNO1* strains grew equally as well under all concentrations of NTC added. This shows that deletion and overexpression of *YNO1* do not have an equal and opposite effect on sensitivity to error-inducing drugs.

Both observations are compatible with the fact that intracellular ROS levels are the same between the wild-type and *ΔYNO1* strains, but higher in the *YNO1* overexpression strain. Perhaps the response to NTC is linked to the ROS that Yno1p produces? 0.1mM hydrogen peroxide increases sensitivity to errors, just like *YNO1* overexpression does. This also aligns itself with the stress-response and adaptation hypotheses outlined earlier.

Combining the NTC and luciferase datasets together, there is a clear link between the very similar effects of *YNO1* and ROS on translational fidelity and response to error-inducing drugs. The exact nature of the relationship is unknown, as they appear to exert their effects to some extent in an independent manner.

The hypothesized potential mechanisms by which Yno1p influences translational fidelity are shown in Figure 20.

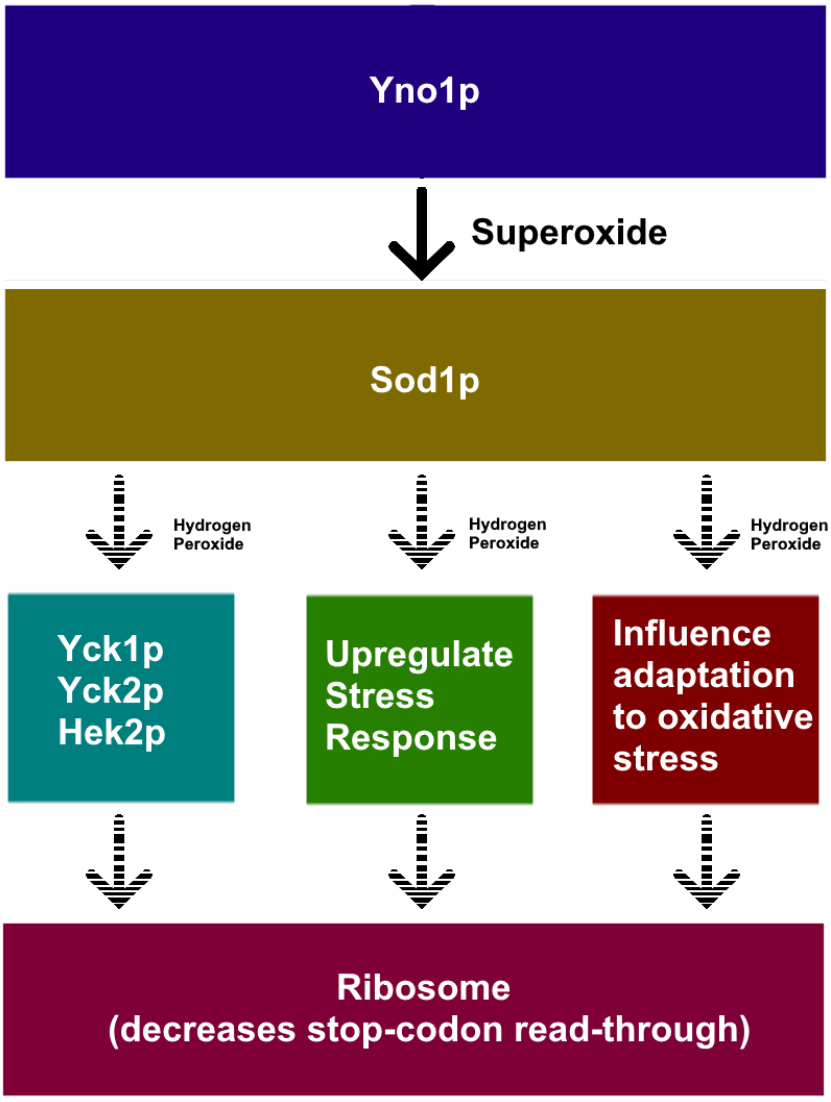

Figure 20: *The possible mechanism(s) through which Yno1p might influence translational fidelity*

Yno1p produces superoxide, which is immediately utilised by Sod1p. Sod1p then has three possible pathways it could interact with. One involves Yck1p, Yck2p and Hek2p. Another could be to upregulate the stress response through entering the nucleus as a transcription factor. The final is to influence the cell to adapt to high oxidative stress conditions. These will most likely be mediated by hydrogen peroxide. These will then all influence the ribosome in some unknown capacity to act to decrease stop-codon read-through.

Bold lines represent confirmed interactions. Dashed lines represent hypothesized interactions.

4.3 Further experimentation

The evidence gathered here opens up a variety of other hypotheses to test, and would benefit from further experimentation in certain areas too.

The lack of being able to use apocynin as a specific Yno1p inhibitor still leaves open another possibility for inhibiting Yno1p activity to see if it's the copy number or rate of catalyzed reactions per cell which is causing the observed effects. Mutagenesis could be carried out on the active site of *YNO1*; however, the active site of enzymes is very sensitive to change, and so this will be a trial-and-error process with a large possibility with each permutation to destabilize the whole molecule.

The relationship between *YNO1* and ROS should be investigated. Luciferase assays and growth curves should be repeated in the presence of n-acetyl cysteine (NAC). NAC is a precursor to antioxidants enzymes, and therefore aids in reducing the presence of cellular ROS (Sun, 2010). If the effect on stop-codon read-through or NTC sensitivity by *YNO1* is abrogated, then it is indeed global ROS that is the mediator. Otherwise, it is local ROS production immediately delivered to a signalling partner (Reddi and Culotta, 2013) or another function of *YNO1* that is causing the effect. To further bolster these observations all experiments should be repeated in a SOD1 deletion strain, as SOD1 is the presumed immediate downstream signalling enzyme that processes superoxide produced by Yno1p (Reddi and Culotta, 2013).

NTC should be added to cells in a luciferase assay to try and determine which specific markers of fidelity it makes worse; this will help elucidate the currently mysterious relationship between YNO1 and NTC in relation to absolute growth rate.

SOD1 is known to be a transcription factor; under oxidative stress conditions, SOD1 translocates to the nucleus to upregulate the oxidative stress response (Tsang *et al.*, 2015). It is possible that under *YNO1* overexpression conditions SOD1 could be carrying out this role, and the resulting oxidative stress response is what exerts the effect of translational accuracy or NTC sensitivity.

BioGRID (BioGRID, 2018) also has many other deletion strains to subject to experimentation to further elucidate which molecules are required for *YNO1* to exert its effect on fidelity.

As error levels remain constant across the lifespan of the cell, it would be interesting to see what would befall the fidelity measures if *YNO1* was overexpressed in cells of different chronological age.

4.4 In summary

YNO1 is an important regulator of stop-codon read-through, and presents itself as the, or one of the, major methods through which fidelity is maintained throughout the lifetime of the cell. Although the mechanism of action remains unknown, with only a link to ROS production and *YCK1, YCK2* and *HEK2* known for certain, Yno1p promises to be a significant enzyme for further investigation into the relationship between fidelity and ageing.

5 Bibliography

Abbott, J. A., Francklyn, C. S. and Robey-Bond, S. M. (2014) 'Transfer RNA and human disease', *Frontiers in Genetics*, 5, pp. 1–18. doi: 10.3389/fgene.2014.00158.

Atkins, J. F. (1991) 'Towards a genetic dissection of the basis of triplet decoding, and its natural subversion: programmed reading frame shifts and hops', *Annual Reviews Genetics*, 25, pp. 201–228.

Atkins, J. F. and Bjork, G. R. (2009) *A Gripping Tale of Ribosomal Frameshifting: Extragenic Suppressors of Frameshift Mutations Spotlight P-Site Realignment*, *Microbiology and Molecular Biology Reviews*. doi: 10.1128/MMBR.00010-08.

Ayer, A., Gourlay, C. W. and Dawes, I. W. (2014) 'Cellular redox homeostasis, reactive oxygen species and replicative ageing in Saccharomyces cerevisiae', *FEMS Yeast Research*, 14(1), pp. 60–72. doi: 10.1111/1567-1364.12114.

Azpurua, J. *et al.* (2013) 'Naked mole-rat has increased translational fidelity compared with the mouse, as well as a unique 28S ribosomal RNA cleavage', *Proceedings of the National Academy of Sciences USA*, 110(43), pp. 17350–17355. doi: 10.1073/pnas.1313473110.

Belin, S. *et al.* (2009) 'Dysregulation of ribosome biogenesis and translational capacity is associated with tumor progression of human breast cancer cells.', *PLOS One*, 4(9), p. e7147. doi: 10.1371/journal.pone.0007147.

Bertram, G. *et al.* (2000) 'Terminating eukaryote translation: domain 1 of release factor eRF1 functions in stop codon recognition.', *RNA*, 6(9), pp. 1236–1247. doi:

10.1017/S1355838200000777.

BioGRID (2018) *AIM14 Results Summary*. Available at: https://thebiogrid.org/33093/summary/saccharomyces-cerevisiae/aim14.html.

Bucciantini, M. *et al.* (2002) 'Inherent toxicity of aggregates implies a common mechanism for protein misfolding diseases', *Nature*, 416(6880), pp. 507–511. doi: 10.1038/416507a.

Buttgereit, F. and Brand, M. D. (1995) 'A hierarchy of ATP-consuming processes in mammalian cells', *Biochemical Journal*, 312(1), pp. 163–167. doi: 10.1042/bj3120163.

Chiu, J. and Dawes, I. W. (2012) 'Redox control of cell proliferation', *Trends in Cell Biology*, 22(11), pp. 592–601. doi: 10.1016/j.tcb.2012.08.002.

Conn, C. S. and Qian, S.-B. (2013) 'Nutrient Signaling in Protein Homeostasis: An Increase in Quantity at the Expense of Quality', *Science Signaling*, 6(271), pp. ra24-ra24. doi: 10.1126/scisignal.2003520.

Cross, F. R. (1997) '"Marker swap" plasmids: Convenient tools for budding yeast molecular genetics', *Yeast*, 13(7), pp. 647–653. doi: 10.1002/(SICI)1097-0061(19970615)13:7<647::AID-YEA115>3.0.CO;2-#.

Cuesta, R., Gupta, M. and Schneider, R. J. (2009) 'The regulation of protein synthesis in cancer', *Prog Mol Biol Transl Sci*, 90(09), pp. 255–292. doi: S1877-1173(09)90007-2 [pii]\n10.1016/S1877-1173(09)90007-2.

Dekel, E. and Alon, U. (2005) 'Optimality and evolutionary tuning of the expression level of a protein', *Nature*, 436(7050), pp. 588–592. doi: 10.1038/nature03842.

Demeshkina, N. *et al.* (2012) ‘A new understanding of the decoding principle on the ribosome’, *Nature*. 484(7393), pp. 256–9. doi: 10.1038/nature10913.

Denisenko, O. and Bomsztyk, K. (2002) ‘Yeast hnRNP K-like genes are involved in regulation of the telomeric position effect and telomere length.’, *Molecular and cellular biology*, 22(1), pp. 286–97. doi: 10.1128/MCB.22.1.286.

Dever, T. E. and Green, R. (2012) ‘The elongation, termination, and recycling phases of translation in eukaryotes’, *Cold Spring Harbor Perspectives in Biology*, 4(7), pp. 1–16. doi: 10.1101/cshperspect.a013706.

Dever, T. E., Kinzy, T. G. and Pavitt, G. D. (2016) ‘Mechanism and Regulation of Protein Synthesis in Saccharomyces cerevisiae.’, *Genetics*. Genetics, 203(1), pp. 65–107. doi: 10.1534/genetics.115.186221.

Drummond, D. A. and Wilke, C. O. (2008) ‘Mistranslation-induced protein misfolding as a dominant constraint on coding-sequence evolution’, *Cell*, 134(2), pp. 341–352. doi: 10.1038/nrm2621.

Drummond, D. A. and Wilke, C. O. (2009) ‘The evolutionary consequences of erroneous protein synthesis’, *Nature Reviews Genetics*, 10(10), pp. 715–724. doi: 10.1038/nrg2662.

Dua, K. (2001) ‘Translational control of the proteome: Relevance to cancer’, *Proteomics*, 1, pp. 1191–1199.

Farabaugh, P. J. (2000) ‘Translational frameshifting: implications for the mechanism of translational frame maintenance’, *Progress in nucleic acid research and molecular biology*, 64, pp. 131–170. doi: 10.1016/S0079-6603(00)64004-7.

Farabaugh, P. J. and Björk, G. R. (1999) ‘How translational accuracy influences reading frame maintenance.’, *The EMBO journal*, 18(6), pp. 1427–1434. doi: 10.1093/emboj/18.6.1427.

Francklyn, C. S. (2008) ‘DNA Polymerases and Aminoacyl-tRNA Synthetases: Shared Mechanisms for Ensuring the Fidelity of Gene Expression’, *Biochemistry*, 47(45), pp. 11695–11703. doi: 10.1021/bi801500z.DNA.

Gallant, J. *et al.* (1997) ‘The error catastrophe theory of aging. Point counterpoint.’, *Experimental gerontology*, 32(3), pp. 333–46.

Gerashchenko, M. V, Lobanov, A. V and Gladyshev, V. N. (2012) ‘Genome-wide ribosome profiling reveals complex translational regulation in response to oxidative stress.’, *Proceedings of the National Academy of Sciences of the United States of America*. National Academy of Sciences, 109(43), pp. 17394–9. doi: 10.1073/pnas.1120799109.

Gromadski, K. B. and Rodnina, M. V. (2004) ‘Kinetic Determinants of High-Fidelity tRNA Discrimination on the Ribosome’, *Molecular Cell*, 13(2), pp. 191–200. doi: 10.1016/S1097-2765(04)00005-X.

Guo, H. H., Choe, J. and Loeb, L. A. (2004) ‘Protein tolerance to random amino acid change’, *Proceedings of the National Academy of Sciences*, 101(25), pp. 9205–9210. doi: 10.1073/pnas.0403255101.

von der Haar, T. (2008) ‘A quantitative estimation of the global translational activity in logarithmically growing yeast cells’, *BMC Systems Biology*, 2(1), p. 87. doi: 10.1186/1752-0509-2-87.

von der Haar, T. *et al.* (2017) ‘The control of translational accuracy is a determinant of healthy

ageing in yeast.', *Open biology*, 7(1), p. 160291. doi: 10.1098/rsob.160291.

von der Haar, T. (2018) *Preparation and Transformation of Competent E. coli cells (CCMB80 Method)*, *protocols.io*. Available at: dx.doi.org/10.17504/protocols.io.hayb2fw (Accessed: 12 February 2019).

Harley, C. B. *et al.* (1980) 'Protein synthetic errors do not increase during aging of cultured human fibroblasts.', *Proceedings of the National Academy of Sciences of the United States of America*. National Academy of Sciences, 77(4), pp. 1885–9.

Harman, D. (2003) 'The Free Radical Theory of Ageing', *Antioxidants & Redox Signalling*, 5(5), pp. 557–561.

Hinnebusch, A. G. (2014) 'The Scanning Mechanism of Eukaryotic Translation Initiation', *Annual Review of Biochemistry*, 83(1), pp. 779–812. doi: 10.1146/annurev-biochem-060713-035802.

Hopfield, J. J. (1974) 'Kinetic Proofreading: A New Mechanism for Reducing Errors in Biosynthetic Processes Requiring High Specificity', *Proceedings of the National Academy of Sciences USA*, 71(10), pp. 4135–4139. doi: 10.1073/pnas.71.10.4135.

Ibba, M. and Söll, D. (2000) 'Aminoacyl-tRNA Synthesis', *Annual Review of Biochemistry*, 69, pp. 617–50.

Invitrogen (2005) 'ChargeSwitch® Plasmid Yeast Mini Kit', *Invitrogen*.

Jørgensen, F. and Kurland, C. G. (1990) 'Processivity errors of gene expression in Escherichia coli.', *Journal of Molecular Biology*, 215(4), pp. 511–21. doi: 10.1016/S0022-2836(05)80164-0.

Katz, M. J. *et al.* (2016) 'Hydroxylation and translational adaptation to stress: Some answers lie

beyond the STOP codon', *Cellular and Molecular Life Sciences*, 73(9), pp. 1881–1893. doi: 10.1007/s00018-016-2160-y.

Ke, Z. *et al.* (2017) 'Translation fidelity coevolves with longevity', *Aging Cell*, pp. 1–6. doi: 10.1111/acel.12628.

Keeling, K. *et al.* (2004) 'Leaky termination at premature stop codons antagonizes nonsense-mediated mRNA decay in S . cerevisiae Leaky termination at premature stop codons antagonizes nonsense-mediated mRNA decay in S . cerevisiae', *RNA*, 10(4), pp. 691–703. doi: 10.1261/rna.5147804.facilitates.

Kim, S. Y. *et al.* (2012) 'Anti-inflammatory effects of apocynin, an inhibitor of NADPH oxidase, in airway inflammation', *Immunology and Cell Biology*. Nature Publishing Group, 90(4), pp. 441–448. doi: 10.1038/icb.2011.60.

Kochupurakkal, B. S. and Iglehart, J. D. (2013) 'Nourseothricin N-Acetyl Transferase: A Positive Selection Marker for Mammalian Cells', *PLoS ONE*. Edited by G. Almeida-Porada. Public Library of Science, 8(7), p. e68509. doi: 10.1371/journal.pone.0068509.

Kourie, J. I. and Henry, C. L. (2002) 'Ion channel formation and membrane-linked pathologies of misfolded hydrophobic proteins: The role of dangerous unchaperoned molecules', *Clinical and Experimental Pharmacology and Physiology*, 29(9), pp. 741–753. doi: 10.1046/j.1440-1681.2002.03737.x.

Kramer, E. B. *et al.* (2010) 'A comprehensive analysis of translational missense errors in the yeast Saccharomyces cerevisiae A comprehensive analysis of translational missense errors in the yeast Saccharomyces cerevisiae', *RNA*, 16, pp. 1797–1808. doi:

10.1261/rna.2201210.Aminoacylation.

Kramer, E. B. and Farabaugh, P. J. (2007) 'The frequency of translational misreading errors in E. coli is largely determined by tRNA competition.', *RNA*, 13(1), pp. 87–96. doi: 10.1261/rna.294907.

LaRiviere, F. J. (2001) 'Uniform Binding of Aminoacyl-tRNAs to Elongation Factor Tu by Thermodynamic Compensation', *Science*, 294(5540), pp. 165–168. doi: 10.1126/science.1064242.

Leadsham, J. E. *et al.* (2013) 'Loss of cytochrome c oxidase promotes ras-dependent ros production from the ER resident NADPH oxidase, Yno1p, in yeast', *Cell Metabolism*. Elsevier Inc., 18(2), pp. 279–286. doi: 10.1016/j.cmet.2013.07.005.

Lee, J. W. *et al.* (2006) 'Editing-defective tRNA synthetase causes protein misfolding and neurodegeneration', *Nature*, 443(7107), pp. 50–55. doi: 10.1038/nature05096.

Ling, J., Roy, H. and Ibba, M. (2007) 'Mechanism of tRNA-dependent editing in translational quality control.', *Proceedings of the National Academy of Sciences of the United States of America*, 104(1), pp. 72–77. doi: 10.1073/pnas.0606272104.

López-Otín, C. *et al.* (2013) 'The hallmarks of aging', *Cell*, 153(6), pp. 1194–1217. doi: 10.1016/j.cell.2013.05.039.

Machery-Nagel (2017) 'PCR clean-up Gel extraction User Manual'.

Maehigashi, T. *et al.* (2014) 'Structural insights into +1 frameshifting promoted by expanded or modification-deficient anticodon stem loops', *Proceedings of the National Academy of Sciences*,

111(35), pp. 12740–12745. doi: 10.1073/pnas.1409436111.

Manickam, N. *et al.* (2016) 'Effects of tRNA modification on translational accuracy depend on intrinsic codon-anticodon strength', *Nucleic Acids Research*, 44(4), pp. 1871–1881. doi: 10.1093/nar/gkv1506.

Mesquita, A. *et al.* (2010) 'Caloric restriction or catalase inactivation extends yeast chronological lifespan by inducing H2O2 and superoxide dismutase activity', *Proceedings of the National Academy of Sciences*, 107(34), pp. 15123–15128. doi: 10.1073/pnas.1004432107.

Mitkevich, V. A. *et al.* (2006) 'Termination of translation in eukaryotes is mediated by the quaternary eRF1•eRF3•GTP•Mg2+ complex. The biological roles of eRF3 and prokaryotic RF3 are profoundly distinct', *Nucleic Acids Research*, 34(14), pp. 3947–3954. doi: 10.1093/nar/gkl549.

Mohler, K. and Ibba, M. (2017) 'Translational fidelity and mistranslation in the cellular response to stress.', *Nature microbiology*, 2, p. 17117. doi: 10.1038/nmicrobiol.2017.117.

Nauseef, W. M. (2008) 'Biological roles for the NOX family NADPH oxidases.', *The Journal of biological chemistry*. American Society for Biochemistry and Molecular Biology, 283(25), pp. 16961–5. doi: 10.1074/jbc.R700045200.

Ninio, J. (1975) 'Kinetic amplification of enzyme discrimination', *Biochimie*, 57(5), pp. 587–595. doi: 10.1016/S0300-9084(75)80139-8.

Noller, H. (2006) 'Biochemical characterization of the ribosomal decoding site', *Biochimie*, 88(8), pp. 935–941. doi: 10.1016/j.biochi.2006.04.006.

Ogle, J. M. *et al.* (2002) 'Selection of tRNA by the ribosome requires a transition from an open to a closed form', *Cell*, 111(5), pp. 721–732. doi: 10.1016/S0092-8674(02)01086-3.

Orgel, L. E. (1970) 'The maintenance of the accuracy of protein synthesis and its relevance to ageing', *Proceedings of the National Academy of Sciences of the United States of America*, 67(3), p. 1476. doi: 10.1073/pnas.67.3.1476.

Paquin, N. *et al.* (2007) 'Local Activation of Yeast ASH1 mRNA Translation through Phosphorylation of Khd1p by the Casein Kinase Yck1p', *Molecular Cell*, 26(6), pp. 795–809. doi: 10.1016/j.molcel.2007.05.016.

Parker, J. (1989) 'Errors and alternatives in reading the universal genetic code.', *Microbiological reviews*, 53(3), pp. 273–98. Available at: http://pubmedcentralcanada.ca/pmcc/articles/PMC372737/pdf/microrev00042-0009.pdf%0Ahttp://www.pubmedcentral.nih.gov/articlerender.fcgi?artid=372737&tool=pmcentrez&rendertype=abstract.

Pestova, T. V. and Kolupaeva, V. G. (2002) 'The roles of individual eukaryotic translation initiation factors in ribosomal scanning and initiation codon selection', *Genes and Development*, 16(22), pp. 2906–2922. doi: 10.1101/gad.1020902.

Pestova, T. V *et al.* (2000) 'The joining of ribosomal subunits in eukaryotes requires eIF5B.', *Nature*, 403(6767), pp. 332–335. doi: 10.1038/35002118.

Plant, E. P. *et al.* (2007) 'Differentiating between Near- and Non-Cognate Codons in Saccharomyces cerevisiae', *PLoS ONE*, 2(6), p. e517. doi: 10.1371/journal.pone.0000517.

QIAgen (2015) 'QIAprep® Spin Miniprep Kit'.

Rao, R. V and Bredesen, D. E. (2004) 'Misfolded proteins, endoplasmic reticulum stress and neurodegeneration', *Current Opinions in Cell Biology*, 16(6), pp. 653–662. doi: 10.1016/j.ceb.2004.09.012.

Reddi, A. R. and Culotta, V. C. (2013) 'SOD1 Integrates Signals from Oxygen and Glucose to Repress Respiration', *Cell*, 152(1–2), pp. 224–235. doi: 10.1007/978-1-62703-673-3.

Ribas de Pouplana, L. *et al.* (2014) 'Protein mistranslation: Friend or foe?', *Trends in Biochemical Sciences*, 39(8), pp. 355–362. doi: 10.1016/j.tibs.2014.06.002.

Rinnerthaler, M. *et al.* (2012) 'Yno1p/Aim14p, a NADPH-oxidase ortholog, controls extramitochondrial reactive oxygen species generation , apoptosis , and actin cable formation in yeast', *Proceedings of the National Academy of Sciences*, 109(22), pp. 8658–8663. doi: 10.1073/pnas.1201629109/-DCSupplemental.www.pnas.org/cgi/doi/10.1073/pnas.1201629109.

Rodnina, M. V. *et al.* (2005) 'Recognition and selection of tRNA in translation', *FEBS Letters*, 579(4), pp. 938–942. doi: 10.1016/j.febslet.2004.11.048.

Rodnina, M. V. and Wintermeyer, W. (2009) 'Recent mechanistic insights into eukaryotic ribosomes', *Current Opinion in Cell Biology*, 21(3), pp. 435–443. doi: 10.1016/j.ceb.2009.01.023.

Ross, C. A. and Poirier, M. A. (2004) 'Protein aggregation and neurodegenerative disease', *Nature Medicine*, 10(7), pp. S10–S17. doi: 10.1038/nm1066.

Ross, C. A. and Poirier, M. A. (2005) 'What is the role of protein aggregation in neurodegeneration?', *Nature Reviews Molecular Cell Biology*, 6(11), pp. 891–898. doi: 10.1038/nrm1742.

Rötig, A. (2011) ‘Human diseases with impaired mitochondrial protein synthesis’, *Biochimica et Biophysica Acta (BBA) - Bioenergetics*. Elsevier B.V., 1807(9), pp. 1198–1205. doi: 10.1016/j.bbabio.2011.06.010.

Rozov, A. *et al.* (2015) ‘Structural insights into the translational infidelity mechanism’, *Nature Communications*. Nature Publishing Group, 6, p. 7251. doi: 10.1038/ncomms8251.

Rozov, A. *et al.* (2016) ‘New Structural Insights into Translational Miscoding’, *Trends in Biochemical Sciences*. Elsevier Ltd, 41(9), pp. 798–814. doi: 10.1016/j.tibs.2016.06.001.

Rubenstein, E. (2008) ‘Misincorporation of the proline analog azetidine-2-carboxylic acid in the pathogenesis of multiple sclerosis: a hypothesis.’, *Journal of neuropathology and experimental neurology*, 67(11), pp. 1035–40. doi: 10.1097/NEN.0b013e31818add4a.

Salas-Marco, J. and Bedwell, D. M. (2004) ‘GTP Hydrolysis by eRF3 Facilitates Stop Codon Decoding during Eukaryotic Translation Termination GTP Hydrolysis by eRF3 Facilitates Stop Codon Decoding during Eukaryotic Translation Termination’, *Molecular and Cellular Biology*, 24(17), pp. 7769–7778. doi: 10.1128/MCB.24.17.7769.

Salas-Marco, J. and Bedwell, D. M. (2005) ‘Discrimination between defects in elongation fidelity and termination efficiency provides mechanistic insights into translational readthrough’, *Journal of Molecular Biology*, 348(4), pp. 801–815. doi: 10.1016/j.jmb.2005.03.025.

Schmeing, T. M. *et al.* (2009) ‘The Crystal Structure of the Ribosome Bound to EF-Tu and Aminoacyl-tRNA’, *Science*, 326(5953), pp. 688–694. doi: 10.1126/science.1179700.

Schosserer, M. *et al.* (2015) ‘Methylation of ribosomal RNA by NSUN5 is a conserved mechanism modulating organismal lifespan’, *Nature Communications*, 6(1), p. 6158. doi:

10.1038/ncomms7158.

Schubert, U. *et al.* (2000) ‘Rapid degradation of a large fraction of newly synthesized proteins by proteasomes.’, *Nature*, 404(6779), pp. 770–774. doi: 10.1038/35008096.

Shoemaker, C. J. and Green, R. (2011) ‘Kinetic analysis reveals the ordered coupling of translation termination and ribosome recycling in yeast’, *Proceedings of the National Academy of Sciences*, 108(51), pp. E1392–E1398. doi: 10.1073/pnas.1113956108.

Sievers, A. *et al.* (2004) ‘The ribosome as an entropy trap’, *Proceedings of the National Academy of Sciences*, 101(21), pp. 12397–12398.

Sigma (2019) *Nourseothricin sulfate*. Available at: https://www.sigmaaldrich.com/catalog/product/sigma/74667?lang=en&region=GB (Accessed: 12 February 2019).

sittingpretty.us (2018) *96 Well Template*. Available at: http://sittingpretty.us/img/src/96-well-plate-template/96-well-plate-template-carisoprodolpharm-com-f5nLuhN0JU.jpg (Accessed: 21 June 2018).

Söll, D. (1990) ‘The Accuracy of Aminoacylation - Ensuring the Fidelity of the Genetic Code’, *Experientia*, 46, pp. 1089–1096. doi: 10.1007/BF01936918.

Soto, C. (2003) ‘Unfolding the role of protein misfolding in neurodegenerative diseases’, *Nature Reviews Neuroscience*, 4(1), pp. 49–60. doi: 10.1038/nrn1007.

Stahl, G. *et al.* (2004) ‘Translational accuracy during exponential, postdiauxic, and stationary growth phases in Saccharomyces cerevisiae.’, *Eukaryotic cell*. American Society for

Microbiology (ASM), 3(2), pp. 331–8. doi: 10.1128/EC.3.2.331-338.2004.

Stansfield, I. *et al.* (1998) 'Missense translation errors in Saccharomyces cerevisiae', *Journal of Molecular Biology*, 282(1), pp. 13–24. doi: http://dx.doi.org/10.1006/jmbi.1998.1976.

Stefani, M. and Dobson, C. M. (2003) 'Protein aggregation and aggregate toxicity: New insights into protein folding, misfolding diseases and biological evolution', *Journal of Molecular Medicine*, 81(11), pp. 678–699. doi: 10.1007/s00109-003-0464-5.

Stoebel, D. M., Dean, A. M. and Dykhuizen, D. E. (2008) 'The cost of expression of Escherichia coli lac operon proteins is in the process, not in the products', *Genetics*, 178(3), pp. 1653–1660. doi: 10.1534/genetics.107.085399.

Sun, S.-Y. (2010) 'N-acetylcysteine, reactive oxygen species and beyond.', *Cancer biology & therapy*, 9(2), pp. 109–10.

Tsang, C. K. *et al.* (2015) 'Superoxide dismutase 1 acts as a nuclear transcriptional factor to regulate oxidative stress resistence', *Nat Commun*, 5(3446). doi: 10.1038/ncomms4446.Superoxide.

Warner, J. R. (1999) 'The economics of ribosome biosynthesis in yeast', *Trends in Biochemical Sciences*, 24(11), pp. 437–440. doi: 10.1016/S0968-0004(99)01460-7.

Wells, S. E. *et al.* (1998) 'Circularization of mRNA by Eukaryotic Translation Initiation Factors', *Molecular Cell*, 2(1), pp. 135–140. doi: 10.1016/S1097-2765(00)80122-7.

Zaher, H. S. and Green, R. (2009a) 'Fidelity at the Molecular Level: Lessons from Protein Synthesis', *Cell*, 136(4), pp. 746–762. doi: 10.1016/j.cell.2009.01.036.

Zaher, H. S. and Green, R. (2009b) ‘Quality control by the ribosome following peptide bond formation’, *Nature*. Nature Publishing Group, 457(7226), pp. 161–166. doi: 10.1038/nature07582.

Zenklusen, D., Larson, D. R. and Singer, R. H. (2008) ‘Single-RNA counting reveals alternative modes of gene expression in yeast’, *Nature Structural & Molecular Biology*, 15(12), pp. 1263–1271. doi: 10.1038/nsmb.1514.Single-RNA.

Zhang, Y. *et al.* (2009) ‘Mice Deficient in Both Mn Superoxide Dismutase and Glutathione Peroxidase-1 Have Increased Oxidative Damage and a Greater Incidence of Pathology but No Reduction in Longevity’, *The Journals of Gerontology Series A: Biological Sciences and Medical Sciences*, 64A(12), pp. 1212–1220. doi: 10.1093/gerona/glp132.

Zhao, L. *et al.* (2005) ‘Protein accumulation and neurodegeneration in the woozy mutant mouse is caused by disruption of SIL1, a cochaperone of BiP’, *Nature Genetics*, 37(9), pp. 974–979. doi: 10.1038/ng1620.